A conserved role for Notch in priming the cellular response to Shh through ciliary localisation of the key Shh transducer, Smoothened.

Magdalena Stasiulewicz, Shona Gray, Ioanna Mastromina, Joana Clara Silva, Mia Bjorklund, Philip A. Seymour[†], David Booth, Calum Thompson, Rich Green, Emma A. Hall[$], Palle Serup[†], J. Kim Dale[*]

Division of Cell and Developmental Biology, College of Life Sciences, University of Dundee, Dow Street, Dundee DD1 5EH, Scotland, UK. . [†]The Danish Stem Cell Center, Faculty of Health Sciences, University of Copenhagen, Blegdamsvej 3B, DK-2200, Copenhagen, Denmark. [$] MRC Human Genetics, Institute for Genetics and Molecular Medicine, University of Edinburgh, Edinburgh, EH4 2XU.

[*]Corresponding author: j.k.dale@dundee.ac.uk

Tel : +44 01382 386290

Fax: +44 01382 385386

Abstract

Notochord-derived Sonic Hedgehog (SHH) is essential for dorso-ventral patterning of the overlying neural tube. Increasing concentration and duration of Shh signal induces progenitors to acquire progressively more ventral fates. We show Notch signalling augments the response of neuroepithelial cells to Shh, leading to the induction of higher expression levels of the Shh target gene Ptc1 and subsequently induction of more ventral cell fates. Furthermore, we demonstrate activated Notch1 leads to pronounced accumulation of Smo within primary cilia and elevated levels of full-length Gli3. Finally, we show Notch activity promotes longer primary cilia both in vitro and in vivo. Strikingly, these Notch-regulated effects are Shh-independent. These data identify Notch signalling as a novel modulator of Shh signalling which acts mechanistically via regulation of ciliary localisation of key components of its transduction machinery.

Key Words: Notch, SHH, embryo, chick, mouse, cilia, notochord, floor plate, P3 progenitors

Introduction

The notochord is the source of a signal, Sonic Hedgehog (Shh) that patterns the dorsoventral aspect of the neural tube (Echelard et al., 1993; Krauss et al., 1993; Marti et al., 1995). The response of neural progenitors is dependent on both the concentration and duration of Shh signalling to which they are exposed (reviewed in Cohen et al., 2013; Briscoe and Novitch, 2008; Briscoe and Therond 2013). This leads to the induction and spatial distribution of distinct transcription factors in different progenitor pools along the dorsal-ventral axis of the neural tube. The most ventral populations are floor plate and p3 progenitors (which will give rise to V3 interneurons). In the absence of Shh signalling these cell types do not develop. Floor plate induction initially requires exposure to a high burst of Shh but full floor plate maturation requires these cells then attenuate their response to Shh (Ribes et al., 2010). In contrast, maintenance of Shh signalling is required for the full differentiation of the p3 progenitors.

It is well established that Shh signal transduction requires primary cilia (Huangfu et al., 2003; reviewed in Sasai and Briscoe, 2012). In the absence of Shh ligand, the transmembrane receptor patched (PTC) is located in the base of the cilia and represses the pathway by binding and inhibiting the ciliary localisation of smoothened (SMO) (Taipale et al., 2002; (Rohatgi et al., 2009, Rohatgi et al., 2007, Sasai and Briscoe, 2012; Chen et al., 2011; Milenkovic et al., 2009; Stamataki et al., 2005, Briscoe and Therond, 2013). Activation of the pathway is achieved by binding of Shh to PTC, which releases the inhibition on SMO allowing it to translocate into the cilia. Smo prevents proteolytic cleavage of the Gli transcription factors, so that full-length Gli translocates to the nucleus to activate target gene transcription. It is possible that other signalling pathways may interact with the Shh pathway by regulating ciliary translocation of these key transduction components.

The Notch pathway plays a key role in various aspects of patterning and cell fate choice during neurogenesis (Henrique et al., 1995; Louvi and Artavanis-Tsakonas 2006; Pierfelice et al., 2011; Hori et al., 2013; Guruharsha 2012), such as balancing numbers of progenitor cells with that of differentiating neurons through lateral inhibition/specification (Henrique et al., 1995; Pierfelice et al., 2011) and regulating binary cell fate choice of progenitors as they differentiate into different neuronal subtypes (Okigawa et al., 2014). Both receptor and ligands are membrane bound proteins so the pathway is activated by cell-cell communication. Upon activation by the Delta/Serrate ligands in adjacent cells, the Notch receptor undergoes a number of proteolytic cleavage events, the last of which is mediated by a γ-secretase enzyme complex which cleaves the intracellular domain of Notch (NICD). NICD translocates to the nucleus where it binds to the obligate transcription factor of the pathway, RBPJ, and creates a dual binding interface for Mastermind-like (MAML) family of proteins

which are essential components of the transcriptional activation complex. This ternary complex is essential for transcriptional activation of Notch target genes.

Recent reports have demonstrated enrichment of Notch signalling components in primary cilia and aberrations in ciliogenesis impact on activation of the Notch pathway (Leitch et al., 2014; Ezratty et al., 2011). Despite extensive studies on the role of Shh and Notch pathways in patterning and development of the central nervous system, and the intriguing fact primary cilia mediate efficient signalling for both pathways (at least in some contexts), nothing is known about the potential crosstalk between these pathways during establishment of the dorso-ventral pattern of progenitor domains across the neural tube.

Here we report a novel role for Notch in augmenting the response of neural progenitors to Shh in the chick and mouse neural tube and provide insight into the establishment of floor plate and P3 identity. Using gain and loss of function assays, we show that Notch is required for cells to acquire the most ventral cell fate in response to Shh but that attenuation of Notch signalling is equally important for these cells to fully differentiate as floor plate. Strikingly, we show Notch activation promotes Shh-independent accumulation of Smo within cilia, leads to elevated levels of full-length Gli3 and formation of longer cilia. Together, the data suggest Notch acts mechanistically to prime neural progenitor cells to respond to Shh through changing ciliary architecture and localisation of Smo to the cilia.

Methods

Chick embryo

White Leghorn *Gallus gallus* eggs (Henry Stewart & Co, Lincolnshire and Winter Farm, Royston) or GFP-expressing embryos (Roslin Institute, Midlothian (McGrew et al., 2004)) were incubated at 38.5°C in a humidified incubator to yield embryos between Hamburger Hamilton (HH) stages 5 and 17 according to Hamburger and Hamilton, 1992.

Mouse embryo

Wild-type CD1 mouse (Mus musculus) embryos were obtained at E8.5- E11.5 days dpc, fixed for immunohistochemistry or in situ hybridisation. Genotyping of Rosa26^{dnMaml1} (Horn et al., 2012), *Foxa2*^{mcm} (Park et al., 2008), Rosa26$^{LSL\text{-}NICD}$ (Murtaugh et al., 2003), *Psen1*$^{-/-}$*; Psen2*$^{-/-}$ (Donoviel et al., 1999), *RBPjK -/-* (Oka et al., 1995) and *Rosa26*$^{LSL\text{-}YFP}$ (Srinivas et al., 2001) was done using PCR. Rosa26^{dnMaml1} and *RBPjK -/-* mice were kept as heterozygotes. Foxa2^{mcm}Rosa26$^{LSL\text{-}NICD}$ embryos were obtained by crossing *Foxa2*^{mcm} male with Rosa26$^{LSL\text{-}NICD}$ female. Pregnant females were administered 8mg of tamoxifen (Sigma, T5648) by oral gavage, at E7.5 and E8.5 dpc and embryos were collected at E10.5 or alternatively at E6.5 and E7.5 dpc and embryos were collected at E9.5.

Cell culture

NIH-3T3 mouse and DF1 chick fibroblasts were cultured in a humidified incubator and maintained at 37 °C in an atmosphere of 5% CO_2, in Dulbecco's modified Eagle's medium (DMEM; Life technologies) supplemented with 10% heat inactivated Newborn Calf Serum (NBCS; Life Technologies) or Foetal Bovine Serum (FBS, Sigma), respectively. Cells were transfected using Lipofectamine LTX with Plus Reagent Kit (Invitrogen) either with control empty plasmid (PCIG; Megason and McMahon, 2002), PCIG-NICD or pCIG-cHairy2 (Dale et al., 2003) at final concentration of 1 µg/ml. For ciliated cell enrichment, transfected cells were maintained 24 hours in DMEM supplemented with 0.5% NBCS or 0.5% FBS for NIH3T3 and DF1, respectively (that enriches for cells in G1 which is when cilia formation occurs predominantly) (Basten SG, Giles RH., 2013) before treating with 4 nM recombinant ShhN protein (University of Dundee) for 12 hours.

Explant culture

Explants isolated from HH stage 6-7 chick embryos were cultured in collagen (Placzek and Dale, 1999), in 100 µM γ-secretase inhibitor IX (DAPT) (Calbiochem) dissolved in dimethylsulphoxide (DMSO) (Sigma) or DMSO alone for 36 hours unless stated otherwise. Notochord and intermediate

lateral neural plate (I-LNP) co-culture explants employed notochord from a GFP-transgenic embryo to distinguish neural versus mesodermal expression of FoxA2 and Islet1. Where stated, I-LNP explants were cultured in 1 nM or 4 nM recombinant Shh protein.

Electroporation

pCIG-NICD, pCIG-*cHairy2*, pCIG-dominant-negative *cHairy2* (Broom et al., 2012), or pCIG vectors were introduced to the caudal neural plate of HH10-12 embryos using standard *in ovo* electroporation (Dale et al., 2003; Briscoe et al., 2000). Embryos were cultured overnight before fixation.

***In situ* hybridisation (ISH) and immunohistochemistry**

Standard in situ hybridisation methods were used (Henrique et al., 1995). Embryos were fixed in 4% PFA in PBS at pH 7.2, on ice for 2 hours. Cells growing on coverslips were fixed in 4% PFA in PBS for 15 minutes. For Patched1 antibody, cells were fixed with 2% PFA for 5 minutes followed by 5 minutes of ice cold MeOH at -20^{0}C. Antibody protocols have been described for Foxa2 (1:10), 3B9, Nkx2.2 (1:10), Islet1 (1:10), Shh (1:10; DSHB), Olig2 (1:16,000; generous gift from B.Novitch; California, USA), Aristaless (ARX 1:1000; Jamel Chelly; Paris, France), Arl13b (1:3000; N295B/66, UC Davis/NIH NeuroMa), Smoothened (1:3000 Abcam, ab38686), Patched1 (1:750; University of Dundee), acetylated tubulin (1:1000 SIGMA, T7451), mNICD (1:200; Cell Signaling, D3B8), cNICD (1:2000; University of Dundee), anti-GFP (1:1000; Life Tech, A6455) (Ericson et al., 1996; Ericson et al., 1997; Ericson et al., 1992; Gibb et al., 2009; Yamada et al., 1991, Caspary et al., 2007, Cruz et al., 2010, Bone et al., 2014, Huppert et al., 2005)

Phospho-Histone-H3 immunohistochemistry on explants

Fixed tissue was proteinase K (Roche) -treated and fixed (4% formaldehyde in PBS, 2 mM EGTA, 0.1% glutaraldehyde (Sigma). Anti-phospho-histone-H3 antibody (Upstate) was added at a concentration of 10 µg/ml.

Marker gene analysis in mutant embryos

Cell counts for each marker were performed on sections and expressed as a proportion of the domain covered by the two markers. Heterozygotes provided a characteristic template of neuronal patterning from which comparisons could be made with mutant littermates.

Western Blotting

Western blot analysis was described previously (Bone et al., 2014). 10ug sample was loaded. Gli3 rabbit Antibodies (generous gift of Susan Mackem, Frederick, USA) and mouse anti-tubulin (Abcam) were diluted 1:1000 and 1:5000.

qRT-PCR

Total RNA extracted from the caudal region (below forelimb) of E9.5 Foxa2^{mcm}Rosa26$^{LSL\text{-}NICD}$ using QIAGEN Micro Plus Kit. cDNA synthesised using SuperScript^{TM} III reverse transcriptase (Life Technologies). qRT-PC performed with Power SYBR Mater Mix (Life Technologies), and reactions measured in a C1000 Thermal Cycler (Bio-Rad) with the following conditions: 95^{0}C for 5 min, 40 cycles 95^{0}C for 15 seconds and 60^{0}C for 1 min. *Patched1, Gli1* (Han et al., 2009), *Hes1* (Li et al., 2012) and *cHairy2* primers (F: 5'-CCGTACCCTGCAAGCCAGGTG-3', R: 5'-GCCCATCAGAGGCAAGCAGCA-3') were described previously and normalised against *beta Actin* (Ferjentsik et al., 2009; Ribes et al., 2010) using the Pfaffl equation (Pfaffl, 2001).

Image acquisition/analysis

Fluorescent signal was acquired using a compound microscope (Leica DM5000 B), an Olympus IX70 deconvolution microscope or the Zeiss LSM-710 confocal microscope. Image analysis was carried out in deconvolved pseudo-coloured images using Volocity software or the open access software Fiji.

Statistical analysis

Data analysis was conducted using the open source statistical software R (R Core Team, 2012). Differences in cilia length and PTC cilia intensity were tested using ANOVA on log transformed response data, with post-hoc pairwise comparisons conducted using Tukey Honest Significant Differences test. Differences in smoothened protein localisation in the cilia; in addition to changes in the counts of categories of cells expressing different markers across the anterior-posterior axis of the R26dnMaml1 or control mouse embryos were evaluated using a chi-square test. Plots were generated using R studio, sigma plot and Microsoft Office Excel. Phospho-histone-H3- labelled chromatin in control and treated explants was analysed by ANOVA.

Results.

Notch activation mirrors Shh target gene expression in floor plate and P3 domains.

We previously showed the Notch target gene *cHairy2* is expressed in Hensen's node and axial tissues as they leave the node in HH stage 5-11 chick embryos where it is co-expressed with the earliest floor plate marker, *cFoxa2* (Gray and Dale 2010). As development proceeds *cHairy2* expression in the ventral neural tube mirrors that of the Shh target *Ptc1*, both spatially and temporally: expression is high in the floor plate and P3 progenitor domains in the caudal neuraxis, whereas, in more anterior, developmentally mature regions expression is down-regulated in the floor plate but maintained in the adjacent P3 progenitor domain (Figure 1A-C'; Ribes et al., 2010). Immunohistochemistry for the cleaved activated form of the Notch1 receptor, NICD, in mouse and chick, reveals the profile of NICD production coincides with *cHairy2* expression in the floor plate and P3 domain in addition to the previously reported NICD activity in progenitors lining the lumen of the neural tube (Figure 1D-E'). The Notch target *Hes1*, orthologue of *cHairy2*, is also expressed in the mouse ventral neural tube (data not shown; Sasai et al., 1992; Jouve et al., 2000). Thus, NICD production and *cHairy2/Hes1* expression occur at the right time and place to play a role in floor plate development.

Shh induces *cHairy2* expression in I-LNP in a Notch-dependent manner

To examine whether *c-Hairy2* transcription is Shh-dependent we micro-dissected intermediate lateral neural plate (I-LNP) explants, that would never normally express *c-Hairy2* from HH stage 6 chick embryos and cultured them in the presence/absence of recombinant Shh protein (ShhN). I-LNP alone did not express *c-Hairy2* (*n*=0/3; 2 LNPs per explant; Figure 2A). However, exposure to 4 nM ShhN (the concentration required to induce floor plate markers; Erikson et al., 1996) induced *c-Hairy2* (*n*=12/13; 2 LNPs per explant; Figure 2B). Using the γ-secretase inhibitor DAPT (Dale et al., 2003; Morohashi et al., 2006) to inhibit Notch signalling we found that 50 µM DAPT inhibited Shh induction of *c-Hairy2* (*n*=9/9; 2 LNPs per explant; Figure 2C). Thus, Shh induces *c-Hairy2* in the neuroepithelium in a Notch-dependant manner. This suggests that Shh-dependent onset of *c-Hairy2* expression is part of the response of these midline cells to becoming floor plate.

Notch inhibition prevents notochord induction of FOXA2.

To address whether Notch plays a role in Shh mediated floor plate induction by notochord we micro-dissected HH stage 6 chick I-LNPs and cultured them with a HH stage 6 notochord from GFP-expressing chick embryos. Explants co-cultured in DAPT showed no *cNetrin1* or FOXA2 expression (*n*=12/14 and *n*=5/5 respectively; Figures 2F, 2L) compared to controls (*n*=5/5; Figure 2E; *n*=16/16;

Figure 2K). Surprisingly, DAPT did not affect induction of the motor neuron marker Islet1 (controls *n*=5/5; DAPT *n*=5/5; Figure 2H-I). As expected *cHairy2* was completely lost in floor plate and Hensen's node explants following DAPT treatment (controls *n*=21/22; *n*=20/22: treated *n*=25/25; *n*=16/18 respectively; Supplementary Figure 1A-D). I-LNPs alone failed to express *cNetrin1*, Islet 1 or FOXA2 (*n*=18/18; *n*=32/32, respectively; Figure 2D, G, J). These data suggest Notch is required for notochord-mediated induction of floor plate but not motor neurons.

DAPT did not affect *cBrachyury* (*cT*) or 3B9/cNot1 expression in co-cultures (*n*= 12/13; controls n=14/14; Figure 2M-N and data not shown) or node or notochord only explants (*n*=8/9 and *n*=12/12; controls n=8/8 and 16/16; Supplementary Figure 1G-J). These data indicate Notch acts specifically within the neuroectoderm to modulate the response of this tissue to Shh. Floor plate induction requires a higher dose of Shh than motor neuron induction and in the absence of Notch, the neuroectoderm only displays the low-dose response to Shh.

The TUNEL assay did not reveal a significant difference in apoptotic index between DAPT and control explants (controls *n*=3, DAPT *n*=3; one-way ANOVA; df =1; F=1.235; p = 0.274; Supplementary Figure 2B-B'). However, DAPT explants were visibly smaller, likely due to the significant reduction in the mitotic index (reduced number of phospho-histone H3 labelled cells; controls *n*=2, DAPT *n*=2; Kruskal-Wallis 1-way ANOVA; df =1; H= 14.286; p=<0.001; Supplementary Figure 2A-A'), as expected in the absence of Notch activity.

Notch modifies sensitivity to Shh.

The finding that Notch inhibition blocks floor plate induction could be due to lower Shh production by notochord or a higher concentration of Shh required by the neuroectodermal cells. To distinguish between these possibilities we repeated the assay but substituted notochord with varying concentrations of ShhN protein in the presence/absence of DAPT. Controls cultured in 4 nM ShhN expressed both FOXA2 (*n*=12/12) and Islet1 (*n*=13/13; Figure 2P, T*)*. DAPT abrogated FOXA2 expression (*n*=16/16) but Islet1 persisted *(n*=17/20; Figure 2Q, U). These data recapitulate the results observed with the notochord assay. I-LNP explants cultured in 8 nM ShhN plus DAPT expressed both FOXA2 (*n*=11/15) and Islet1 (*n*= 15/15; Figure 2R, V). Since an excess of ShhN rescued floor plate induction, these data imply Notch acts in neural cells to lower their threshold response to Shh and thereby specify the cell fate they acquire.

***cHairy2* mis-expression leads to dorsal expansion of P3 and early floor plate markers.**

To test whether Notch modifies the threshold concentration of Shh perceived via induction of Shh itself, we electroporated the caudal neural tube of HH stage 10 embryos with pCIG-NICD (pCAAGs vector encoding both a constitutively active form of Notch [Notch intracellular domain, NICD, normally only released following ligand activated γ-secretase cleavage] and GFP, separated by an IRES) or the Notch target *cHairy2* [pCIG-cHairy2], and analysed Shh expression by immunohistochemistry. We observed by in situ hybridisation and qRT-PCR that NICD mis-expression induces ectopic *cHairy2* expression in the neural tube (n=5, 75/93 sections; Supplementary Figure 3 and data not shown). However, neither NICD nor *cHairy2* electroporation altered the endogenous expression profile of Shh (*n*=5, *n*=3 embryos respectively; Figure 3A-C'). To ensure this was not due to cells having lost competence to acquire floor plate characteristics, we electroporated the open neural plate with pCIG-NICD at HH stage 6, cultured the embryos for 6 hours and isolated GFP-positive I-LNP explants then cultured these for 36 hours; again, we saw no Shh induction (*n*=6; Supplementary Figure 3). Thus, Notch signalling does not induce Shh expression.

We tested the hypothesis that *cHairy2* mis-expression in more dorsal regions may induce the differentiation of more ventral characteristics by changing the sensitivity of those cells to the endogenous Shh morphogen gradient. *cHairy2* electroporation led to a dorsal expansion of the domains of FOXA2^{+} cells and Nkx2.2^{+} cells and a concomitant reduction of the domain of Olig2^{+} cells (*n*=2 for each marker pCIG; *n*=6 for each marker *cHairy2*; Figure 3D-L''). Moreover, within the motor neuron progenitor domain, cells which down-regulated Olig2, cell-autonomously up-regulated Nkx2.2, indicating a change of fate from a motor neuron to a p3 progenitor (Figure 3J-L'', *n*=6). Specification of ventral cell types is progressive: midline cells, which constitute the presumptive floor plate, initially express markers common to p3 progenitors, namely FOXA2 and Nkx2.2. Nkx2.2 becomes down-regulated, and late FP markers, including Shh and Arx, are induced (Ribes et al., 2010). We used double immunohistochemistry to determine whether ectopic activation of FOXA2 by mis-expression of cHairy2 is indicative of floor plate or p3 identity. We observed the predominant response was up-regulation of Nkx2.2 (*n*=2 embryos, 90/159 sections) with half those sections co-expressing FOXA2 (47 sections; Figure 3H-I'). In contrast, definitive early floor plate fate (FOXA2 + only), was induced less robustly (Figure 3H-I'').

In a complementary approach we electroporated a dominant-negative form of *cHairy2* (lacking the WRPW domain; Broom et al., 2012) and observed down-regulation of Nkx2.2 in the P3 domain where *cHairy2* is endogenously expressed at this stage (n=2; Supplementary Figure 4). These findings

imply reducing Notch activity can increase the threshold concentration at which neural cells respond to Shh and thereby modify the extent of the expression domains of distinct dorso-ventral markers induced by Shh. In particular, Notch activity, mediated by cHairy2, promotes acquisition of P3 identity, and to a lesser extent, early floor plate identity in response to Shh.

Maintained Notch activity/*cHairy2* expression in ventral midline cells prevents floor plate maturation and promotes P3 identity.

Ptc1 mRNA is only transiently expressed by floor plate since these cells attenuate their response to Shh to acquire full floor plate fate, in contrast to P3 progenitors that require sustained Shh signalling and maintain *Ptc1* expression (Ribes et al., 2010). *cHairy2* expression mirrors that of *Ptc1* in these domains. We tested the hypothesis that *cHairy2* too must be extinguished in ventral midline cells for them to acquire full floor plate fate. Embryos electroporated with *cHairy2* in the ventral midline at HH10 and harvested at HH17 displayed a cell-autonomous exclusion of the mature floor plate marker ARX in targeted cells (*n*=3 embryos, Figure 4A-B') with a concomitant up-regulation of Nkx2.2 in some cases indicating a fate change to P3 identity (Figure 4 A-B'). These data demonstrate *cHairy2* can modulate the response of cells to Shh and imply that *cHairy2* is necessary for the acquisition of ventral cell fate in response to high Shh signal concentration but it also needs to be down-regulated for floor plate cells to fully mature and differentiate. We next investigated whether loss of Notch activity is also necessary for full acquisition of floor plate fate. To achieve this, we used a conditional mouse line in which NICD is persistently expressed in the floor plate (Tamoxifen-inducible mER;Cre;mER recombinase driver line under the control of the Foxa2 promoter ($Foxa2^{mcm}$) crossed with a $R26^{NICDiresGFP}$ line (Murtaugh et al., 2003; Park et al., 2008)). The $R26^{NICDiresGFP}$ strain permits conditional expression of NICD in cells expressing Cre recombinase. Strikingly, in these E9.5 and E10.5 embryos we observed a cell autonomous up-regulation of Nkx2.2 in lineage labelled ventral midline cells (4C-E, G-L') concomitant with a down-regulation of both Foxa2 and ARX (*n*=6 embryos; Figure 4G-L'). These results phenocopy *cHairy2* electroporation in the chick floor plate. They suggest elevated Notch activity is sufficient to maintain competence to respond to Shh in the ventral midline supporting a role for Notch in the induction/maintenance of the p3 fate. Strikingly, qRT-PCR for *Patched1* in caudal neural tissue isolated from E9.5 $R26^{NICDiresGFP}$ embryos revealed *Patched1* mRNA levels were doubled in the neural tube of these embryos (Figure 4F; n=13) as compared to wild type siblings, demonstrating that Notch activity augments the cellular response to Shh.

Notch modifies the cell fate choice of neural progenitors in response to Shh *in vivo*.

To determine whether Notch is necessary for neural tube patterning in response to Shh, we analysed the same progenitor markers in *Presenilin (Psen) Psen1*$^{-/-}$*; Psen2*$^{-/-}$ and *RBPjK -/-* embryos. Presenilin 1 and 2 are the key components of the γ-secretase enzyme complex which cleaves NICD. Thus, *Psen1*$^{-/-}$*; Psen2*$^{-/-}$ embryos lack all Notch signalling, while *RBPjK*$^{-/-}$ embryos lack the obligate transcription factor required for Notch signalling. Both phenotypes are embryonic-lethal at E9.5 (Oka et al., 1995; Donoviel et al., 1999). In both lines, the combined expression domains of FoxA2 and Nkx2.2 in the ventral neural tube were dramatically reduced at E9 (*n*=6 heterozygous controls and *n*=3 *Psen1*$^{-/-}$*; Psen2*$^{-/-}$; *n*=3 heterozygotes and *n*= 3 *RBPjK*$^{-/-}$; Supplementary Figure 5 and data not shown). In *RBPjK*$^{-/-}$ embryos, cell counts showed the domain of the caudal neural tube occupied by FoxA2^{+}/Nkx2.2^{+} cells to be significantly lower than in controls (4% versus 7% in heterozygotes; P<0.001). To examine mutant embryos that survive beyond E9.5 we analysed mice in which the transcriptional activity of Notch is blocked only in ventral midline and P3 progenitors, by FoxA2^{T2AiCre}-induced expression of a dominant-negative Mastermind1-eGFP fusion protein from a targeted *Rosa26* locus (*Rosa26*^{dnMaml1}; Figure 5; High et al., 2008; Tu et al., 2005; Horn et al., 2012; Maillard et al., 2008). Dominant-negative MAMl1 eGFP fusion protein is a potent and specific inhibitor of all four mammalian Notch receptors *in vivo*. *FoxA2*^{T2AiCre}*; Rosa26*^{dnMaml1} embryos analysed at E9 (n=3) revealed that within the combined FoxA2^{+}, Nkx2.2^{+} or FoxA2^{+}/Nkx2.2^{+} domain most cells were FoxA2^{+}/Nkx2.2^{+}, indicative of an immature FP and/or P3 cell type (*n*=5; Figure 5A-B), as compared to controls (Foxa2T2AiCre; Rosa26RYFP stage-matched embryos in which the Cre-recombined cells are normally Notch-sensitive; data not shown). Quantification of these effects revealed a significantly higher proportion of FoxA2^{+}/Nkx2.2^{+} cells and a significantly lower proportion of P3 (Nkx2.2^{+} only) cells (Figure 5I; X^2=50.52 df=1, *n* = 2 3 5 1 c e l l s , *p*=1.068x10^{-11}) The number of FoxA2^{+} only cells is relatively low in both controls and mutants at this developmental stage. E10.5 *FoxA2*^{T2AiCre}*; Rosa26*^{dnMaml1} embryos also showed a significantly different distribution of these three cell types as compared to controls in particular maintaining a higher proportion of FoxA2^{+}/Nkx2.2^{+} cells and a lower proportion of P3 (Nkx2.2^{+} only) and early floor plate cells (FoxA2^{++} only) (Figure 5C-D; X^2=145.66; df=1, *n*=2462 cells , *p*=< 2.2x10^{-16}). At E11.5 a significantly different distribution of cells in these three categories was maintained (Figure 5I; X^2=83.44, df=1, *n*=3151 cells, *p*= < 2.2x10^{-16}); while the proportion of double-positive cells was similar to controls (Figure 5E-F, I), these embryos exhibited a significantly higher proportion of P3 and lower proportion of floor plate cells compared to controls (Figure 5I). Analysis of Arx and Shh expression at E10.5 reveals that this small population of early floor plate cells go on to express late floor plate markers in the absence of Notch (Figure 5G-H and data not shown). These data suggest in the absence of Notch cells are delayed in the adoption

of a P3 or floor plate fate. Eventually this resolves such that significantly fewer cells give the high dose response.

Notch activity regulates localisation of Smo to the primary cilia in a Shh-independent manner

Ciliary localization of Smo is critical for activation of the SHH pathway (Huangfu et al., 2003; reviewed in Sasai and Briscoe 2012). To test whether regulation of Smo localisation might be a mechanism through which Notch activity modulates the efficacy of Shh signalling we used the Shh-responsive NIH-3T3 primary fibroblast cell line. Double-labelling with antibodies to Smo and to acetylated tubulin (which marks stable microtubules found in cilia), revealed a highly significant accumulation of SMO in the cilia of NIH-3T3 cells upon addition of ShhN (Figure 6B, G; X^2=61.19 ,df=1, *n*=157 cells , *p*= 5.16x10^{-15}) whereas, in the absence of ShhN, cilia are largely devoid of SMO (Figure 6A, G) (Rohatgi et al., 2007). Strikingly, activation of Notch, by transfecting NIH-3T3 cells with NICD-pCIG, dramatically and significantly augmented the number of cells showing SMO localization in cilia, in a Shh-independent manner (Figure 6C, G; X^2=41.62, df=1, *n*=139, *p*=1.11x10^{-10}). Addition of ShhN to the NICD-pCIG transfected cells further enhances the effect (Figure 6D, G; X^2=6.56, df=1, *n*=130, *p*=0.01041). To preclude the possibility of a cell-type specific effect we replicated the experiments in chicken DF-1 fibroblast cells by transfecting cells with *cHairy2-pCIG*, to closely mimic the electroporation analysis performed in chick embryos. We observed a very similar phenotype, whereby cHairy2-pCIG transfection dramatically increased the proportion of cells with SMO localisation in cilia, again in a Shh-independent manner (Figure 6H; X^2=7.65, *df*=1, *n*=116, *p*=0.00565). The further addition of ShhN augmented this effect (Figure 6H; X^2=9.36, *df*=1, *n*=73, *p*=0.002212). In the absence of Shh, PTC inhibits SMO localisation in primary cilia. Double-labelling with antibodies to PTC and Arl13b (a small GTPase that localise to cilia (Caspary et al., 2007) we measured intensity of PTC staining in cilia of NIH-3T3 cells and saw a dramatic reduction when we added ShhN, as expected (Supplementary Figure 6). To address if Notch modulates this effect we treated NIH-3T3 cells with 150 nM LY411575, a γ-secretase inhibitor, which abolished *Hes1* mRNA expression, as expected (Figure 6F; Ferjentsik et al., 2009). Remarkably, Notch inhibition led to a highly significant dampening of PTC clearance from cilia in response to ShhN (*n*=2 replicates; 1205 cells). These data are reflected in the significant post-hoc pairwise comparisons using the Tukey HSD test (F(2, 1205)=176.5, *p*=< 0.001; Supplementary Figure 6). Taken together, these data demonstrate that Notch activity has a conserved, Shh-independent and significant effect upon localisation of key components of the Shh pathway within primary cilia, functioning at the level of PTC/SMO interface to modulate ciliary localisation of these two signalling components.

Notch signalling regulates the level of full-length Gli3 in NIH-3T3 cells.

Full activation of SMO is a two-step process and ciliary transport is the initial requirement (Rohatgi et al., 2009, Rohatgi et al., 2007, Sasai and Briscoe, 2012; Chen et al., 2011; Milenkovic et al., 2009). Within cilia, SMO can exist both in an inactive state and in the phosphorylated-active form. The latter prevents proteolytic cleavage of the Gli transcription factors which then translocate to the nucleus to replace the cleaved repressor form and activate transcription of target genes (Stamataki et al., 2005, Briscoe and Therond, 2013). Addition of 4 nM ShhN to NIH-3T3 fibroblasts leads to a sharp reduction in levels of Gli3R (*n*=3; Figure 6E; Humke et al., 2010; Niewiadomski et al., 2014). We did not observe a concomitant increase in levels of full-length Gli3, likely due to the fact this highly labile transcriptional activator undergoes rapid nuclear translocation, phosphorylation, and destabilization (Humke et al., 2010). In contrast, exposure to NICD-pCIG or Hes1-pCIG alone led to an increase in the levels of full-length Gli3, in NIH-3T3 fibroblasts (*n*= 3 replicates; Figure 6E and data not shown). This is a striking result given the 20% transfection efficiency (analysed by flow cytometry; data not shown). The addition of both ShhN and NICD-pCIG did not change levels of full-length Gli3 from that seen with NICD/Hes1 alone, although levels of Gli3R were dramatically reduced (*n*= 3 replicates; Figure 6E). These data reveal that concomitant with accumulating Smo protein in cilia, Notch signalling elevates levels of full-length Gli3. We next determined whether loss of Notch would affect Shh target gene transcription in NIH-3T3 fibroblasts. qRT-PCR analysis revealed 150nM LY411575 dramatically reduced ShhN-mediated induction of *Ptc1* and *Gli1* (n=2 replicates; Figure 6F). Notably, ShhN also induced *mHes1* expression in a Notch-dependent fashion, supporting the I-LNP data (Figure 2B). Together these data support the hypothesis that Notch signalling amplifies the cellular response to Shh.

Notch signalling regulates cilia length both in the ventral neural tube and in NIH-3T3 fibroblasts.

An additional striking and unexpected effect of NICD in NIH-3T3 cells is that cilia were significantly longer at the *p*=<0.001 level ([F(2,1534)=128.557, *p*=< $2.2x10^{-16}$; Figure 6C, D compared to A, B; Figure 7A). *In vivo*, previous reports have shown the floor plate cilia become significantly longer than P3 cilia (Cruz et al., 2010; Figure 7). To assess whether the effects of Notch upon ventral neural tube patterning may be associated with changes in cilia length we measured cilia in the floor plate and lateral neural plate in both gain and loss of function transgenic mouse models (*FoxA2*^{T2AiCre}*; Rosa26*^{dnMaml1} and in *Foxa2*^{mcm}*;Rosa26*$^{LSL\text{-}NICD}$ mice). Using Arl13b antibodies we observed that floor plate cilia in *FoxA2*^{T2AiCre}*; Rosa26*^{dnMaml1} embryos are significantly shorter than in control litter mates at E9, E10.5 and E11.5 at the p<0.01 level (E9 *n*=3 embryos, E10.5 *n*=3 embryos, E11.5 *n*=2 embryos;

1354 cells counted; Figure 7C-F; floor plate: p= 0.003682, p< $2.2x10^{-16}$, p< $2.2x10^{-16}$, respectively). These data are reflected in the significant post-hoc pairwise comparisons using the Tukey HSD test in Table 1. In contrast, when we analyse cilia length in the floor plate and P3 domain in gain of function *Foxa2*^{mcm}*;Rosa26*$^{LSL\text{-}NICD}$ mice at E10.5 we observed P3 cilia were significantly longer (0.4 microns more), than in control siblings (n=2 embryos; 249 cells; Figure 7B; p=< $2.2x10^{-16}$; Table 1). Floor plate cilia however, were no different in length compared to controls (Figure 7B; p=0.5624687; Table 1). These observations suggest the mechanism by which Notch modulates the response of cells to Shh may be through regulating both cilia length and localisation of SMO within the cilia.

Discussion:

Primary cilia are important regulators of Shh signal transduction (Sasai and Briscoe 2012). We provide *in vitro* and *in vivo* evidence supporting a novel role for the Notch pathway in modulating ciliary architecture and localisation of Smo to this cell appendage. We propose that this serves as a means to prime cells to respond to the Shh morphogen. *In vivo* this synergistic interaction plays a key part in dorso-ventral patterning of the developing neural tube in both chick and mouse embryos.

Intriguingly, NICD production occurs throughout the dorsoventral axis of the neural tube, yet the Notch target *cHairy2* expression is restricted to the floor plate/P3 domain (and the roof plate), in contrast to the broader expression of other Hes homologues (Fior and Henrique 2005). We propose this is likely due to co-operative activation of *cHairy2* by Shh and Notch in the ventral midline. One possible explanation for how this synergy might operate is that Shh might induce expression of Notch itself or a Notch ligand. Indeed, NICD electroporation in more dorsal regions drives ectopic *cHairy2* expression in the neural tube indicative of the fact that endogenous levels of Notch signalling may be higher in the floor plate. Serrate 1 is a potential candidate in this respect as it is expressed in the ventral midline of the chick and mouse neural tube at early developmental stages (JKD unpublished data; le Roux I, et al., 2003).

Paradoxically, we have shown previously DAPT treatment of whole embryos completely blocked *cHairy2*, but did not alter FOXA2 expression (Gray and Dale 2010), whereas we show here DAPT treatment of I-LNPs blocks Shh induction of both *cHairy2* and FOXA2. However, in the whole embryo assay we demonstrated a larger notochord forms from node progenitors in the absence of Notch. This increase in the number of Shh-producing cells and potentially the levels of Shh was proposed to mediate the induction of FOXA2 expression/floor plate characteristics in the absence of Notch. In support of that idea, we show in this study rescue of FOXA2 in the absence of Notch by simply increasing concentration of Shh to which the I-LNP is exposed.

We use a wide variety of gain- and loss-of-function approaches in both chicken and mouse to show interactions between Notch and Shh are critical for dorsal-ventral cell fate specification in the neural tube. Inhibiting Notch signalling impedes floor plate induction while ectopic Notch activation in more dorsal regions ventralises those cells. After floor plate induction, Notch signalling is normally down-regulated in the ventral midline, and forced maintenance prevents floor plate maturation, resulting in the formation of more P3 progenitors in both chick and mouse. This novel role for Notch is very different to the well-established role for Notch in maintaining neural progenitors and preventing their differentiation. We provide multiple lines of evidence these effects are due to

Notch modulating progenitor cell interpretation of the Shh spatiotemporal gradient rather than directly regulating cell fate or differentiation: first the *in vitro* I-LNP assay shows Notch inhibition changes sensitivity but not competence of cells to respond to Shh; second the *FoxA2*^{T2AiCre}*; Rosa26*^{dnMaml1} embryos show a temporal delay in competence to respond to Shh; third Notch modulation of SMO/PTC trafficking to cilia, levels of Gli3 and Shh target gene expression in vivo and vitro directly demonstrates Notch affects progenitor cell interpretation/response to Shh. While the dorso-ventral patterning output of this Notch/Shh synergistic interaction has not been previously reported, an intriguing parallel with our findings is that, in zebrafish lateral floor plate progenitors, loss of Notch leads to loss of Hh response and initiation of Kolmer-Agduhr interneuron differentiation (Huang et al., 2012), although the mechanism governing this synergistic interaction remains unknown.

We show part of this mechanism relies on the subcellular localisation of the key Shh signalling component SMO; NICD mis-expression *in vitro* dramatically augments the initial step of ciliary accumulation of SMO, in a Shh-independent manner. This effect is phenocopied by cHairy2 and thus is likely to be a transcriptional response. The identification of the NICD/cHairy2 target gene involved in trafficking Smo to the cilia will require further investigation.

In addition, NICD mis-expression led to elevated levels of full-length Gli3 *in vitro*. This might be due to Notch promoting inhibition of the cleavage of full-length Gli to the repressor form directly or indirectly through increasing accumulation of SMO in cilia, and/or this may be a transcriptional response, given that Gli2 and Gli3 have previously been reported to be direct targets of N1ICD/RBPJ (Li et al., 2012). As expected, exposure to ShhN dramatically lowers levels of Gli3R, both in the presence/absence of NICD, which is not phenocopied by exposure to NICD alone. These data suggest NICD-mediated ciliary accumulation of SMO and elevated levels of full-length Gli3 are not sufficient to stimulate full activation of the Shh pathway. Rather, we propose these events prime cells to respond efficiently and in a timely fashion when they become exposed to Shh.

An additional unexpected and Shh-independent effect of NICD activation within NIH-3T3 fibroblasts was the formation of significantly longer primary cilia. This effect on ciliary length is also evident *in vivo* in transgenic lines which serve to activate or inhibit Notch activity specifically in the ventral midline. This effect is likely to be transcriptionally regulated since it is observed in *FoxA2*^{T2AiCre}*; Rosa26*^{dnMaml1} embryos. A recent report demonstrated that supernumery cilia reduced Shh pathway transcriptional activation (Mahjoub MR, and Stearns T., 2012). In contrast, within the neural tube of *Arl13b* mutants that form cilia half the length of normal cilia, there is a failure to induce dorso-

ventral markers characteristic of the highest levels of Shh signalling, although expression of genes that require lower levels of Shh signalling continue to be expressed (Caspary et al., 2007). Thus, Shh signalling is sensitive to cilia length, number and architecture. It has previously been shown cilia length changes within the ventral midline of the developing neural tube during normal development (Cruz et al., 2010). Thus, floor plate cilia become almost double the length of those in the adjacent lateral neural tube and this has been associated with Shh-dependent onset of *FoxJ1* expression within the floor plate (Cruz et al., 2010). Indeed FoxJ1 mis-expression is sufficient (but not necessary) for longer cilia in the neural tube. In a variety of developmental contexts Foxj1 has been associated with production of motile cilia that are considerably longer than primary cilia (Cruz et al., 2010; Blatt et al., 1999; Chen et al., 1998; Stubbs et al., 2008; Tichelaar et al., 1999; Yu et al., 2008). A previous report linking Notch signalling to ciliary architecture came from zebrafish (Lopes et al., 2010). Kupffer's vesicle is enriched with long motile cilia, whose function is key for onset of left-right asymmetry. Lopes et al., showed Notch signalling directly regulates ciliary length, and inefficiencies in Notch signal transduction result in shorter cilia and aberrations in left-right asymmetry. One target of Notch in this regard is Foxj1 (Lopes et al., 2010). Thus it is possible that Foxj1 mediates the NICD-dependent changes to ciliary architecture in the ventral neural tube. Intriguingly, Cruz et al suggest FoxJ1 attenuates the response to Shh and that this is cilia-dependent. It is noteworthy however that the subcellular localisation of SMO is not affected by *Foxj1* misexpression, indicating that NICD-mediated changes in cilia length and SMO localisation might be differentially-regulated (Cruz et al., 2010). Indeed, we did not observe changes in cilia length following cHairy2 or Hes1 mis-expression, indicating this effect is mediated by a different set of Notch target effectors. Thus, our working model proposes that NICD activity leads to both increased ciliary length and ciliary localisation of SMO, by two independent mechanisms, which together prime the cell for an accentuated response to the Shh ligand.

The delay in acquisition of ventral fates seen in neural progenitors expressing dnMAMl1-eGFP indicates a potential role for Notch in regulating the temporal response to Shh. It is well established the spatiotemporal pattern of ventral marker induction in the neural tube reflects changes in both concentration and duration of Shh signalling over time. Our data invoke a model in which the role of Shh-dependent Notch activity is to prime cells to respond efficiently and appropriately to Shh by increasing length of cilia and accumulation of SMO within these structures, thereby facilitating rapid Shh-triggered activation of SMO once ligand is received.

In conclusion, our findings using both *in vitro* and *in vivo* models reveal a conserved and novel mechanism to refine and modulate the response repertoire and cell sensitivity to Shh during tissue development. This role for Notch may also affect a broad range of other pathways reliant on ciliary localisation of signalling components in a wide variety of developmental and disease contexts.

Acknowledgments

We are grateful to JKD laboratory. Special thanks go to I Jones, M. C. Jørgensen for experimental assistance, to K. Storey, M Maroto for critical reading of the manuscript. We thank B.Novitch for communication prior to submission and J. Briscoe, O. Pourquie, M Stavridis, R Kageyama, J Chelly for reagents; Marianne Reilly, Nikoletta Patourgia for administrative support. This work was supported by a BBSRC studentship to MS; CRUK studentship to IM; MRC project grant to JKD; a Welcome Trust Strategic award **097945/Z/11/Z.** PS was funded by the Novo Nordisk Foundation.

Author Contribution Statement:

JKD developed the concepts/approach, performed some experiments and prepared the manuscript. MS and SG designed and performed the majority of experiments, all data analysis and preparation of figures. IM performed cell culture. DB performed statistical analyses. PS collected/genotyped *FoxA2*^{T2AiCre}*; Rosa26*^{dnMaml1} embryos. MS, IM, PS, Palle Serup edited the manuscript. JCS performed QRT-PCR. MB gave technical assistance. EH performed cell culture. CT performed cryosectioning. RG performed double in situ hybridisation.

References

Ahnfelt-Rønne J, Hald J, Bødker A, Yassin H, Serup P, Hecksher-Sørensen J. (2007) "Preservation of proliferating pancreatic progenitor cells by Delta-Notch signaling in the embryonic chicken pancreas." BMC Dev Biol. 7:63.

Allen BL, Song JY, Izzi L, Althaus IW, Kang JS, Charron F, Krauss RS, McMahon AP (2011) "Overlapping roles and collective requirement for the coreceptors GAS1, CDO, and BOC in SHH pathway function." Dev Cell 20: 775-787

Balaskas N, Ribeiro A, Panovska J, Dessaud E, Sasai N, Page KM, Briscoe J, Ribes V (2012) "Gene regulatory logic for reading the Sonic Hedgehog signaling gradient in the vertebrate neural tube." Cell 148: 273-284

Basak O, Giachino C, Fiorini E, Macdonald HR, Taylor V. (2012) "Neurogenic subventricular zone stem/progenitor cells are Notch1-dependent in their active but not quiescent state." J Neurosci. 32(16):5654-66.

Basten SG, Giles RH. (2013) "Functional aspects of primary cilia in signaling, cell cycle and tumorigenesis." Cilia. 29;2(1):6. doi: 10.1186/2046-2530-2-6

Blatt, E. N., Yan, X. H., Wuerffel, M. K., Hamilos, D. L. and Brody, S. L. (1999). "Forkhead transcription factor HFH-4 expression is temporally related to ciliogenesis." Am. J. Respir. Cell Mol. Biol. 21, 168-176.

Bone RA, Bailey CS, Wiedermann G, Ferjentsik Z, Appleton PL, Murray PJ, Maroto M, Dale JK (2014). "Spatiotemporal oscillations of Notch1, Dll1 and NICD are coordinated across the mouse PSM." Development 141(24):4806-16.

Bray, S. J. (2006) "Notch signalling: a simple pathway becomes complex." Nat Rev Mol Cell Biol, 7, 678-89.

Briscoe J, Pierani A, Jessell TM, Ericson J. (2000) "A homeodomain protein code specifies progenitor cell identity and neuronal fate in the ventral neural tube." Cell.101(4):435-45

Briscoe J, Novitch BG (2008) "Regulatory pathways linking progenitor patterning, cell fates and neurogenesis in the ventral neural tube." Philos Trans R Soc Lond B Biol Sci. 363(1489):57-70.

Briscoe J, Thérond PP. (2013) "The mechanisms of Hedgehog signalling and its roles in development and disease." Nat Rev Mol Cell Biol. 14(7):416-29

Broom ER, Gilthorpe JD, Butts T, Campo-Paysaa F, Wingate RJ (2012) “The roof plate boundary is a bi-directional organiser of dorsal neural tube and choroid plexus development.” Development 139: 4261-4270

Chen, J., Knowles, H. J., Hebert, J. L. and Hackett, B. P. (1998). Mutation of the mouse hepatocyte nuclear factor/forkhead homologue 4 gene results in an absence of cilia and random left-right asymmetry. J. Clin. Invest. 102, 1077-1082.

Chen Y, Yue S, Xie L, Pu XH, Jin T, Cheng SY. (2011) “Dual Phosphorylation of suppressor of fused (Sufu) by PKA and GSK3beta regulates its stability and localization in the primary cilium.” J Biol Chem. 15;286(15):13502-11.

Cho A, Ko HW, Eggenschwiler JT. (2008) “FKBP8 cell-autonomously controls neural tube patterning through a Gli2- and Kif3a-dependent mechanism. “ Dev Biol. 321(1):27-39.

Cohen M, Briscoe J, Blassberg R (2013) “Morphogen interpretation: the transcriptional logic of neural tube patterning.” Curr Opin Genet Dev (4):423-8.

Colas JF, Schoenwolf GC (2001) “Towards a cellular and molecular understanding of neurulation.” Dev Dyn 221: 117-145

Cruz C, Ribes V, Kutejova E, Cayuso J, Lawson V, Norris D, Stevens J, Davey M, Blight K, Bangs F, Mynett A, Hirst E, Chung R, Balaskas N, Brody SL, Marti E, Briscoe J. (2010) “ Foxj1 regulates floor plate cilia architecture and modifies the response of cells to sonic hedgehog signalling” Development 137, 4271-4282

Dale JK, Maroto M, Dequeant ML, Malapert P, McGrew M, Pourquie O. (2003) “Periodic notch inhibition by lunatic fringe underlies the chick segmentation clock.” Nature. 421(6920):275-8.

Dessaud E, McMahon AP, Briscoe J (2008) “Pattern formation in the vertebrate neural tube: a sonic hedgehog morphogen-regulated transcriptional network.” Development 135: 2489-2503

Donoviel DB, Hadjantonakis AK, Ikeda M, Zheng H, Hyslop PS, Bernstein A. (1999) “Mice lacking both presenilin genes exhibit early embryonic patterning defects.” Genes Dev. 13(21):2801-10.

Echelard, Y., Epstein, D. J., St-Jacques, B., Shen, L., Mohler, J., McMahon, J. A. and McMahon, A. P. (1993). “Sonic hedgehog, a member of a family of putative signaling molecules, is implicated in the regulation of CNS polarity.” Cell 75, 1417-1430.

Ericson J, Rashbass P, Schedl A, Brenner-Morton S, Kawakami A, van Heyningen V, Jessell TM, Briscoe J.(1997) “Pax6 controls progenitor cell identity and neuronal fate in response to graded Shh signaling.” Cell. 90(1):169-80.

Ericson J, Morton S, Kawakami A, Roelink H, Jessell TM.(1996) “Two critical periods of Sonic Hedgehog signaling required for the specification of motor neuron identity.” Cell. 87(4):661-73.

Ericson J, Thor S, Edlund T, Jessell TM, Yamada T.(1992) “Early stages of motor neuron differentiation revealed by expression of homeobox gene Islet-1.” Science. 256(5063):1555-60.

Ezratty EJ, Stokes N, Chai S, Shah AS, Williams SE, Fuchs E. (2011) “A role for the primary cilium in Notch signaling and epidermal differentiation during skin development.” Cell. 145(7):1129-41.

Ferjentsik Z, Hayashi S, Dale JK, Bessho Y, Herreman A, De Strooper B, del Monte G, de la Pompa JK, Maroto M (2009) PLoS Genet. 5(9):e1000662

Fior R, Henrique D. (2005) “A novel hes5/hes6 circuitry of negative regulation controls Notch activity during neurogenesis. Dev Biol 15;281(2):318-33.

Gibb S., Zagorska A., Melton K., Tenin G., Vacca I., Trainor P., Maroto M. and Dale JK. (2009). “Interfering with Wnt signalling alters the periodicity of the segmentation clock”. *Dev Biol.* 330(1):21-31

Gray SD, Dale JK (2010) “Notch signalling regulates the contribution of progenitor cells from the chick Hensen's node to the floor plate and notochord.” Development. 137(4):561-8

Guiu J, Shimizu R, D'Altri T, Fraser ST, Hatakeyama J, Bresnick EH, Kageyama R, Dzierzak E, Yamamoto M, Espinosa L, Bigas A (2013) “Hes repressors are essential regulators of hematopoietic stem cell development downstream of Notch signaling. “ J Exp Med 210: 71-84

Guruharsha, K.G., Kankel, M.W. & Artavanis-Tsakonas, S. (2012) “The Notch signalling system: recent insights into the complexity of a conserved pathway.” Nature reviews. Genetics, 13(9), pp.654–666

Hamburger V, Hamilton HL. (1992) “A series of normal stages in the development of the chick embryo. 1951.” Dev Dyn. 195(4):231-72.

Han YG, Kim HJ, Dlugosz AA, Ellison DW, Gilbertson RJ, Alvarez-Buylla A (2009) “Dual and opposing roles of primary cilia in medulloblastoma development.” Nature Medicine 15(9): 1062-1065.

Hatakeyama J, Bessho Y, Katoh K, Ookawara S, Fujioka M, Guillemot F, Kageyama R (2004) "Hes genes regulate size, shape and histogenesis of the nervous system by control of the timing of neural stem cell differentiation." Development 131: 5539-5550

Henrique, D., Adam, J., Myat, A., Chitnis, A., Lewis, J. and Ish-Horowicz,D (1995). "Expression of a Delta homologue in prospective neurons in the chick." Nature 375 787-790

High F., Lu M., Pear W.S., Loomes K.M., Kaestner K.H., Epstein J.A. (2008) "Endothelial expression of the Notch ligand Jagged1 is required for vascular smooth muscle development". Proc Natl Acad Sci USA 105:1955–1959.

Hori K, Sen A, Artavanis-Tsakonas S. (2013) "Notch signaling at a glance." J Cell Sci. 126(Pt 10):2135-40.

Horn S., Kobberup S., Jørgensen M.C., Kalisz M., Klein T., Kageyama R., Gegg M., Lickert H., Lindner J., Magnuson M.A., Kong Y., Serup P., Ahnfelt-Rønne J., Jensen J.N. (2012) "Mindbomb1 is required for pancreatic β-cell formation" Proc Natl Acad Sci U S A. 109(19): 7356–7361.

Huangfu D, Liu A, Rakeman AS, Murcia NS, Niswander L, Anderson KV.(2003) "Hedgehog signalling in the mouse requires intraflagellar transport proteins." Nature. 6;426(6962):83-7.

Huang P, Xiong F, Megason SG, Schier AF (2012) "Attenuation of Notch and Hedgehog signaling is required for fate specification in the spinal cord. "PLoS Genet 8: e1002762

Humke, E., Dorn, K., Milenkovic, L., Scott, M.,Rohatgi, R.,(2010)" The output of Hedgehog signaling is controlled by the dynamic association between Suppressor of Fused and the Gli proteins" Genes Dev. 24: 670-682

Huppert SS, Ilagan MX, De Strooper B, Kopan R. (2005) "Analysis of Notch function in presomitic mesoderm suggests a gamma-secretase-independent role for presenilins in somite differentiation." Dev Cell. 8(5):677-88

Jouve C, Palmeirim I, Henrique D, Beckers J, Gossler A, Ish-Horowicz D, Pourquié O (2000) "Notch signalling is required for cyclic expression of the hairy-like gene HES1 in the presomitic mesoderm." Development. 127(7):1421-9.

Kim, J., Kato, M. & Beachy, P. A. (2009) "Gli2 trafficking links Hedgehog-dependent activation of Smoothened in the primary cilium to transcriptional activation in the nucleus." Proc Natl Acad Sci U S A, 106, 21666-71.

Kopan, R. & Ilagan, M.X.G., (2009) ”The canonical Notch signaling pathway: unfolding the activation mechanism.” Cell, 137(2), pp.216–233.

Krauss S[1], Concordet JP, Ingham PW. (1993). “A functionally conserved homolog of the Drosophila segment polarity gene hh is expressed in tissues with polarizing activity in zebrafish embryos.” Cell. 75(7):1431-44.

le Roux I, Lewis J, Ish-Horowicz D. (2003) “Notch activity is required to maintain floorplate identity and to control neurogenesis in the chick hindbrain and spinal cord. Int J Dev Biol. 47(4):263-72.

Leitch CC, Lodh S, Prieto-Echagüe V, Badano JL, Zaghloul NA.(2014) “Basal body proteins regulate Notch signaling through endosomal trafficking.” J Cell Sci. 127(Pt 11):2407-19.

Li Y, Hibbs MA, Gard AL, Shylo NA, Yun K (2012) “Genome-wide analysis of N1ICD/RBPJ targets in vivo reveals direct transcriptional regulation of Wnt, SHH, and hippo pathway effectors by Notch1.” Stem Cells 30: 741-752

Lopes, S. S., Lourenco, R., Pacheco, L., Moreno, N., Kreiling, J. & Saude, L. (2010) “Notch signalling regulates left-right asymmetry through ciliary length control”. Development, 137, 3625-32.

Louvi A, Artavanis-Tsakonas S (2006) “Notch signalling in vertebrate neural development.” Nat Rev Neurosci 7: 93-102

Mahjoub MR, Stearns T. (2012) “Supernumerary centrosomes nucleate extra cilia and compromise primary cilium signaling.” Curr Biol. 11;22(17):1628-34.

Maillard I, Koch U, Dumortier A, Shestova O, Xu L, Sai H, Pross SE, Aster JC, Bhandoola A, Radtke F, Pear WS (2008) “Canonical notch signaling is dispensable for the maintenance of adult hematopoietic stem cells.” Cell Stem Cell. 2(4):356-66.

Marklund U, Hansson EM, Sundstrom E, de Angelis MH, Przemeck GK, Lendahl U, Muhr J, Ericson J (2010) “Domain-specific control of neurogenesis achieved through patterned regulation of Notch ligand expression.” Development 137: 437-445

Marti, E., Bumcrot, D. A., Takada, R. and McMahon, A. P. (1995) “Requirement of 19K form of Sonic hedgehog for induction of distinct ventral cell types in CNS explants.” Nature 375, 322-325.

McGrew MJ, Sherman A, Ellard FM, Lillico SG, Gilhooley HJ, Kingsman AJ, Mitrophanous KA, Sang H. (2004) “Efficient production of germline transgenic chickens using lentiviral vectors.” EMBO Rep. 5(7):728-33.

Megason SG, McMahon AP. (2002) “A mitogen gradient of dorsal midline Wnts organizes growth in the CNS.” Development. 129(9):2087-98.

Milenkovic L, Scott MP, Rohatgi R. (2009) “Lateral transport of Smoothened from the plasma membrane to the membrane of the cilium.” J Cell Biol. 2;187(3):365-74.

Morohashi Y[1], Kan T, Tominari Y, Fuwa H, Okamura Y, Watanabe N, Sato C, Natsugari H, Fukuyama T, Iwatsubo T, Tomita T. (2006) “C-terminal fragment of presenilin is the molecular target of a dipeptidic gamma-secretase-specific inhibitor DAPT (N-[N-(3,5-difluorophenacetyl)-L-alanyl]-S-phenylglycine t-butyl ester).” J Biol Chem. 281(21):14670-6. Epub 2006 Mar 28.

Myat A, Henrique D, Ish-Horowicz D, Lewis J. (1996) “A chick homologue of Serrate and its relationship with Notch and Delta homologues during central neurogenesis. Dev Biol. 15;174(2):233-47.

Murtaugh LC, Stanger BZ, Kwan KM, Melton DA. (2003) “Notch signaling controls multiple steps of pancreatic differentiation.” Proc Natl Acad Sci U S A. 100(25):14920-5.

Niewiadomski, P., Kong, J., Ahrends, R., Ma, Y., Humke, E., Khan, S., Teruel, M., Novitch, B., Rohatgi, R., (2014) “Gli Protein Activity Is Controlled by Multisite Phosphorylation in Vertebrate Hedgehog Signaling” Cell Reports 6, 168–181

Oka, C., Nakano, T., Wakeham, A., Pompa, J. L. de la, Mori, C., Sakai, T., Kawaichi, M., Shiota, K., Mak, T. M. and Honjo, T. (1995) ”Disruption of the mouse RBP-J kappa gene results in early embryonic death.” Development 121:3291

Okigawa S, Mizoguchi T, Okano M, Tanaka H, Isoda M, Jiang YJ, Suster M, Higashijima S, Kawakami K, Itoh M. (2014) “Different combinations of Notch ligands and receptors regulate V2 interneuron progenitor proliferation and V2a/V2b cell fate determination.” Dev Biol. 391(2):196-206.

Oosterveen T, Kurdija S, Alekseenko Z, Uhde CW, Bergsland M, Sandberg M, Andersson E, Dias JM, Muhr J, Ericson J (2012) “Mechanistic differences in the transcriptional interpretation of local and long-range Shh morphogen signaling.” Dev Cell 23: 1006-1019

Pan Y, Bai CB, Joyner AL, Wang B (2006) “Sonic hedgehog signaling regulates Gli2 transcriptional activity by suppressing its processing and degradation.” Mol Cell Biol 26: 3365-3377

Park,E.J., Sun,X., Nichol,P., Saijoh, Y., Martin,J.F., Moon, A.M. (2008) "System for Tamoxifen-Inducible Expression of Cre-Recombinase From the Foxa2 Locus in Mice" Developmental Dynamics 237:447–453, 2008

Pfaffl MW (2001) "A new mathematical model for relative quantification in rela-time RT-PCR" Nucleic Acids Rec. 1;29(9):e45

Pierfelice T, Alberi L, Gaiano N (2011) "Notch in the vertebrate nervous system: an old dog with new tricks." Neuron 69: 840-855

Placzek M, Dale K. (1999) "Tissue recombinations in collagen gels." Methods Mol Biol. 97:293-304.

R Core Team (2012). "R: A language and environment for statistical computing." R Foundation for Statistical Computing, Vienna, Austria. ISBN 3-900051-07-0, URL http://www.R-project.org/

Ribes V, Balaskas N, Sasai N, Cruz C, Dessaud E, Cayuso J, Tozer S, Yang LL, Novitch B, Marti E, Briscoe J (2010) "Distinct Sonic Hedgehog signaling dynamics specify floor plate and ventral neuronal progenitors in the vertebrate neural tube." Genes Dev 24: 1186-1200

Ribes V, Briscoe J (2009) "Establishing and interpreting graded Sonic Hedgehog signaling during vertebrate neural tube patterning: the role of negative feedback." Cold Spring Harb Perspect Biol 1:

Roelink, H., Porter, J. A., Chiang, C., Tanabe, Y., Chang, D. T., Beachy, P. A. and Jessell, T. M. (1995) "Floor plate and motor neuron induction by different concentrations of the amino-terminal cleavage product of sonic hedgehog autoproteolysis." Cell 81, 445-455

Rohatgi R, Milenkovic L, Scott MP (2007) "Patched1 regulates hedgehog signaling at the primary cilium." Science. 317(5836):372-6.

Rohatgi R, Milenkovic L, Corcoran RB, Scott MP. (2009) "Hedgehog signal transduction by Smoothened: pharmacologic evidence for a 2-step activation process." Proc Natl Acad Sci U S A. 106(9):3196-201.

Sasai, Y., R.Kageyama, Y. Tagawa, R. Shigemoto, and S.Nakanishi.(1992) "Two mammalian helix-loop-helix factors structurally related to Drosophila hairy and Enhancer of split." Genes & Dev. 6:2620-2634

Sasai N, Briscoe J. (2012) “Primary cilia and graded Sonic Hedgehog signaling.” Wiley Interdiscip Rev Dev Biol. 1(5):753-72.

Sasaki H, Hogan BL (1994) “HNF-3 beta as a regulator of floor plate development.” Cell 76: 103-115

Sasaki H, Hui C, Nakafuku M, Kondoh H (1997) “A binding site for Gli proteins is essential for HNF-3beta floor plate enhancer activity in transgenics and can respond to Shh in vitro.” Development 124: 1313-1322

Shirasaki R, Pfaff SL. (2002) “Transcriptional codes and the control of neuronal identity.” Annu Rev Neurosci. 25:251-81

Srinivas S, Watanabe T, Lin CS, William CM, Tanabe Y, Jessell TM, Costantini F. (2000) “Cre reporter strains produced by targeted insertion of EYFP and ECFP into the ROSA26 locus.” BMC Dev Biol. 1:4.

Stamataki D, Ulloa F, Tsoni SV, Mynett A, Briscoe J (2005) “A gradient of Gli activity mediates graded Sonic Hedgehog signaling in the neural tube. Genes Dev 19: 626-641

Stubbs, J. L., Oishi, I., Izpisua Belmonte, J. C. and Kintner, C. (2008). The forkhead protein Foxj1 specifies node-like cilia in Xenopus and zebrafish embryos. Nat. Genet. 40, 1454-1460.

Taipale J, Cooper MK, Maiti T, Beachy PA. (2002) “Patched acts catalytically to suppress the activity of Smoothened.” Nature. 2002 418(6900):892-7.

Tichelaar, J. W., Lim, L., Costa, R. H. and Whitsett, J. A. (1999). “HNF-3/forkhead homologue-4 influences lung morphogenesis and respiratory epithelial cell differentiation in vivo.” Dev. Biol. 213, 405-417.

Tu L., Fang T.C., Artis D., Shestova O., Pross S.E., Maillard I., Pear W.S. (2005) “Notch signaling is an important regulator of type 2 immunity” J Exp Med. 202(8): 1037–1042.

Yamada T, Placzek M, Tanaka H, Dodd J, Jessell TM (1991) “Control of cell pattern in the developing nervous system: polarizing activity of the floor plate and notochord.” Cell 64(3):635-47.

Yu, X., Ng, C. P., Habacher, H. and Roy, S. (2008). “Foxj1 transcription factors are master regulators of the motile ciliogenic program.” Nat. Genet. 40, 1445-1453.

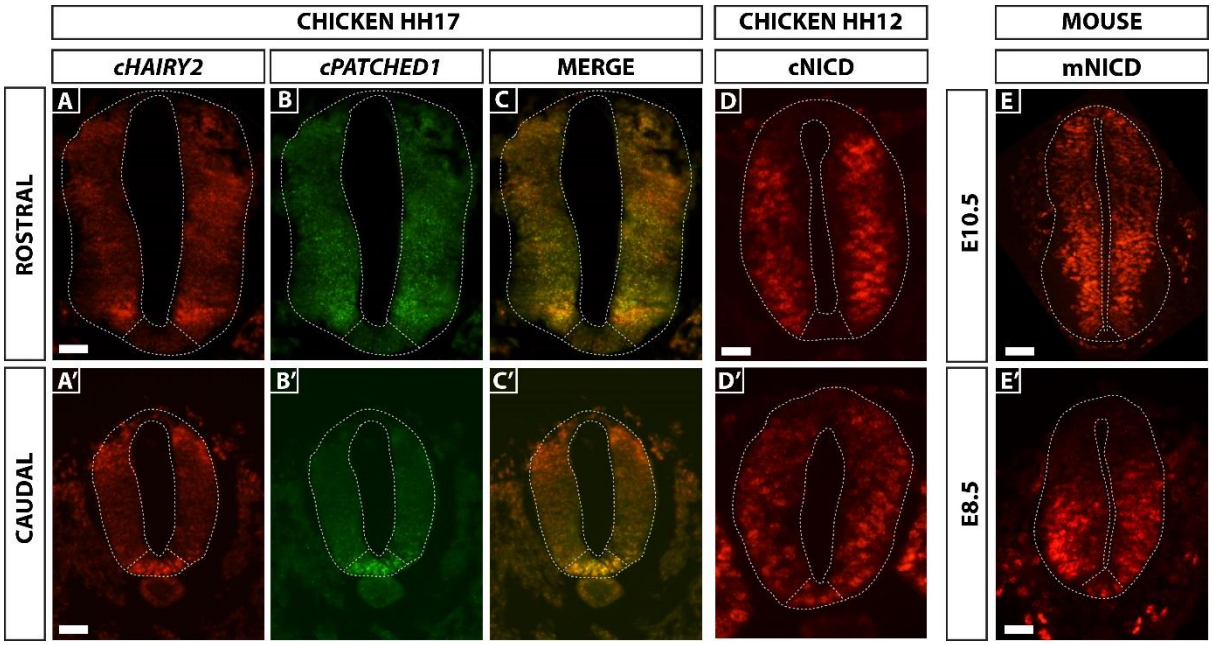

Figure 1. Notch activation mirrors Shh target gene expression in floor plate and P3 domains. A-C' Sections showing *cHairy2* (A-A') and *Patched 1* (B-B') expression in the same neural tube, analysed by fluorescent *in situ* hybridisation (scale bar= 30µm). (D-E') Transverse sections of chick (D-D') and mouse embryos (E-E') showing the profile of NICD by immunohistochemistry (scale bars D= 20µm, E= 50µm, E'= 30µm). (A'-D') Sections through caudal, lumbar regions of the neuraxis. (A-E) Sections through more developmentally mature, brachial regions of the neuraxis. (C-C') Merged images of *cHairy2* and *Patched1* mRNA expression. *cHairy2* is also expressed in more the dorsal neural tube (Broom et al., 2012).

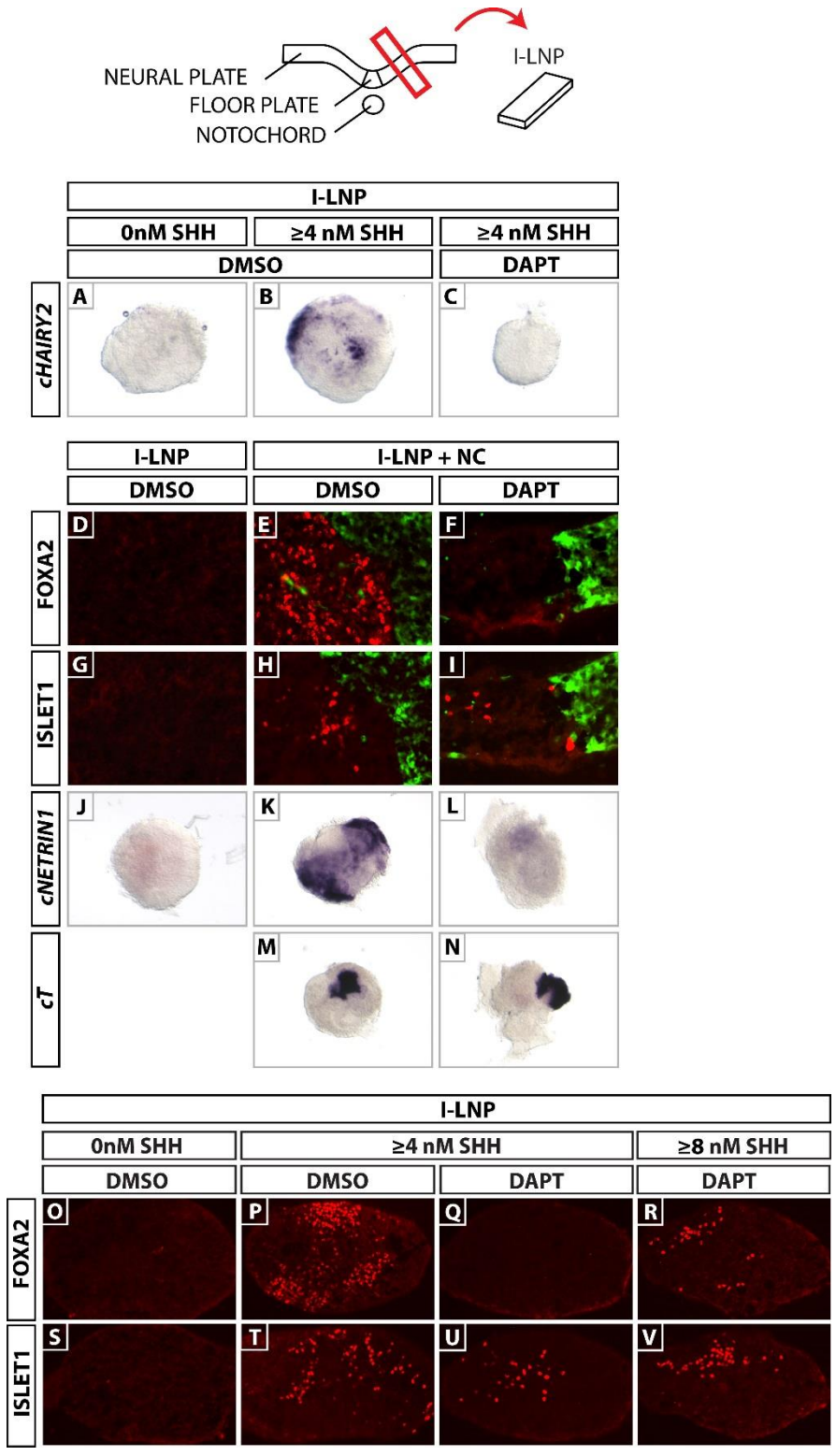

Figure 2. Notch inhibition prevents floor plate but not motor neuron induction by notochord/ShhN.

Schematic of the I-LNP dissection assay. (A) I-LNPs do not express *cHairy2*. (B) ShhN induces *cHairy2* in I-LNP. This is inhibited by DAPT (C). (D-N) I-LNPs cultured alone (D,G,J) or in contact with a GFP^{+}-notochord in DMSO (E,H,K,M) or DAPT (F,I,L,N). Serial sections analysed for FOXA2 or Islet 1 (E and

H, F and I). (D,G, I, M) Isolated I-LNP does not express FOXA2 or Islet 1. Notochord induction of FOXA2 (E) is inhibited by DAPT (F). Islet 1 induction is not affected (H,I). (J) Isolated I-LNP does not express *cNetrin1*. Notochord induction of *cNetrin1* (K) is inhibited by DAPT (L). (M-N) *cT* expression is unaffected by DAPT. (O-V) Sections of I-LNP explants. I-LNP explants cultured in 4 nM ShhN expressed both FOXA2 (P) and Islet1 (T). DAPT exposure prevented FOXA2 expression (Q) but maintained Islet1 (U). I-LNP explants cultured in 8 nM ShhN plus DAPT expressed both FOXA2 (R) and Islet1 (V). I-LNP; intermediate lateral neural plate tissue. *cT*; *cBrachyury*. FP; floor plate.

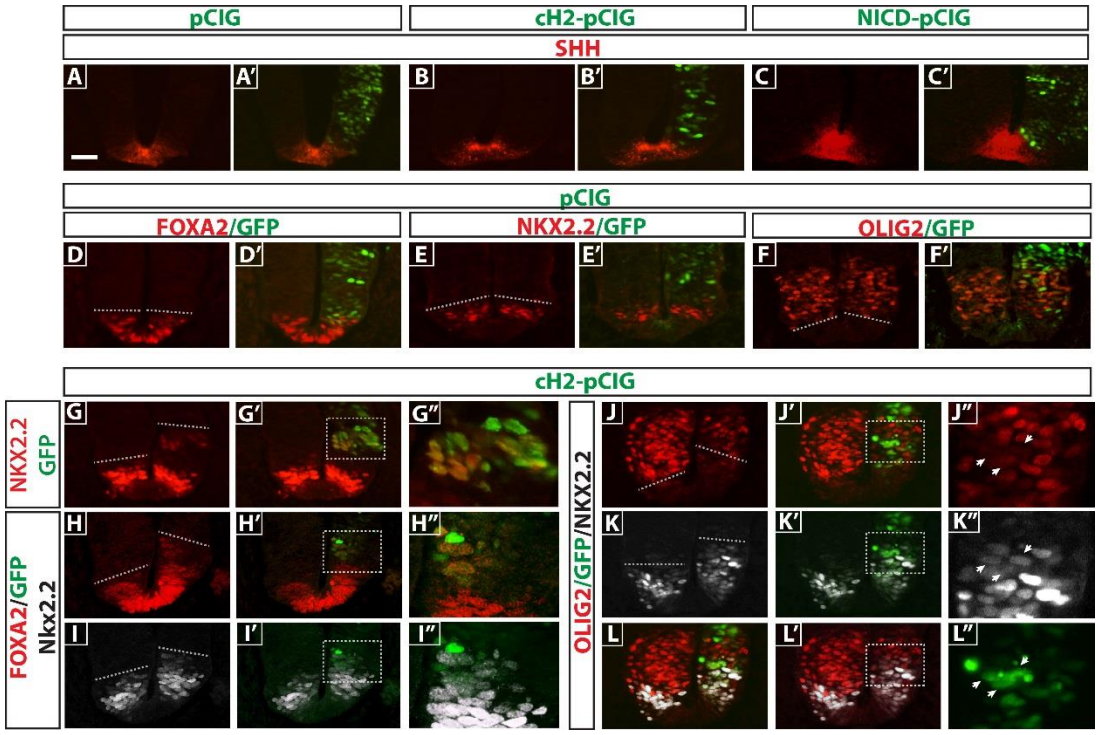

Figure 3. *cHairy2* mis-expression dorsally expands P3 and early floor plate domains. (A-L') Sections of HH 17 chick neural tube 24 hours after electroporation with pCIG (A, A', D, D', E, E', F, F'), pCIG-cHairy2 (B-C', G-L') or 48 hours after pCIG-NICD electroporation (C-C') analysed by immunohistochemistry for GFP (A-L'). Samples were also analysed for Shh (A-B'), FOXA2 (D, D'), Nkx2.2 (E, E', G-G'') or Olig2 (F, F') or double immunohistochemistry for FOXA2 and Nkx2.2 (H-I'') or Olig2 and Nkx2,2 (J-L''). (G''-L'') magnified region of interest in G'-L'. Arrow heads in J''-L'' indicate three cells analysed for GFP, Nkx 2.2 and Olig2. Scale bar = 30µm.

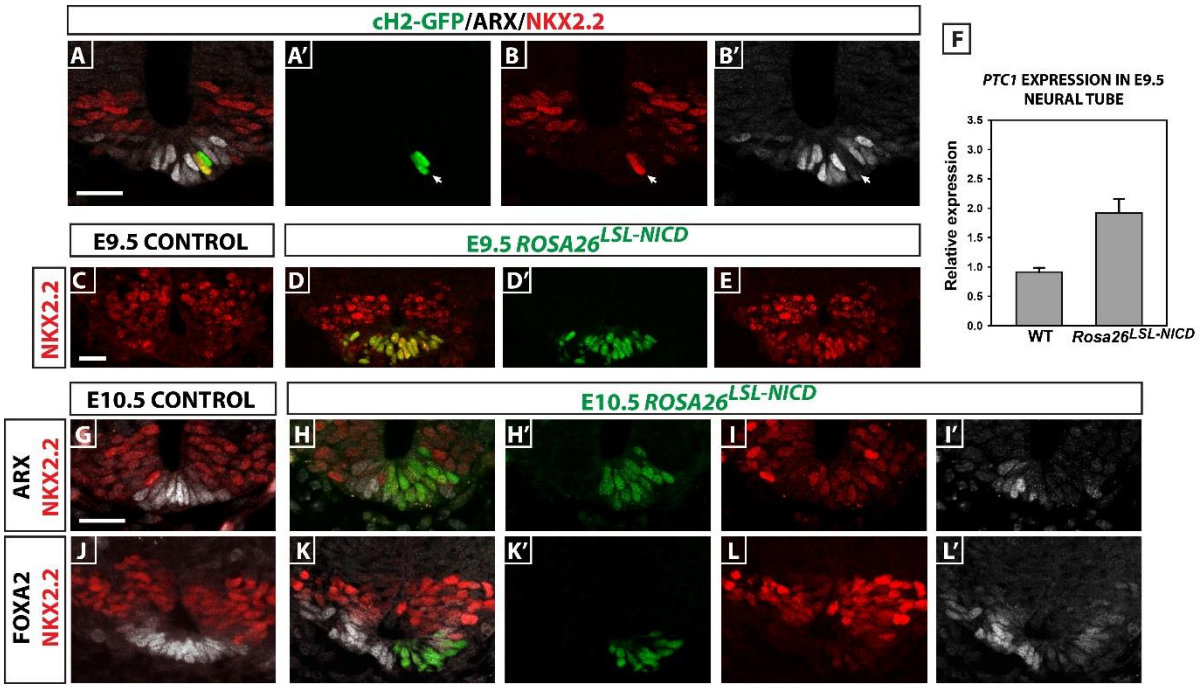

Figure 4. Maintained Notch activity/*cHairy2* expression prevents floor plate maturation and promotes P3 identity. (A-B') Sections of HH 17 neural tube 24 hours after pCIG-cHairy2 electroporation into the ventral midline (cH2-GFP) (scale bar= 15µm). (C-E) Sections of E9.5 *or* (G-L') E10.5 *Foxa2*^{mcm}*;Rosa26*$^{LSL\text{-}NICD}$ embryos (scale bar=30 µm). (A-B', G-I') Sections analysed for GFP, Arx and Nkx2.2 or (C-E) GFP and Nkx2.2 or (J-L') GFP, Foxa2 and Nkx2.2. (F) qRT-PCR analysis of *Patched 1* mRNA levels in E9.5 *Rosa26*$^{LSL\text{-}NICD}$ caudal neural tube compared to wild types.

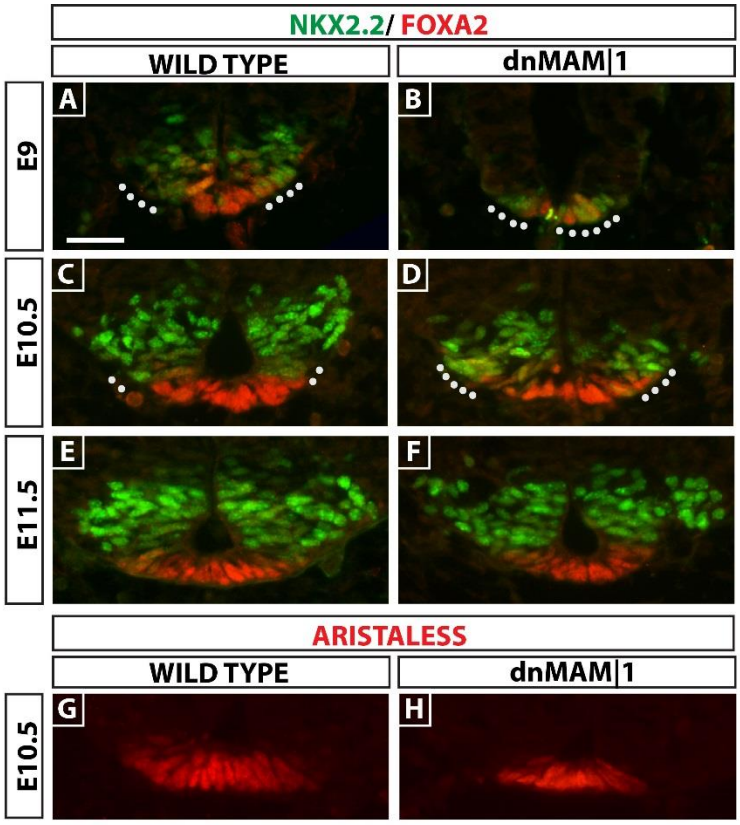

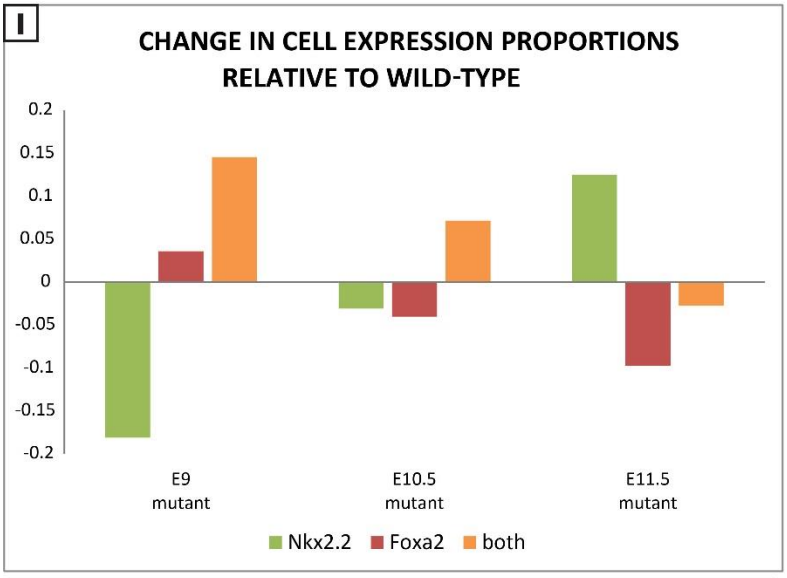

Chisq-test	Mutant E9	Mutant E10.5	Mutant E11.5	WT E9	WT E10.5	WT E11.5
Mutant E9	x	76.0695	304.2513	50.5257	426.2358	157.0166
Mutant E10.5	< 2.2e-16	x	85.82	61.7356	145.6682	40.6917
Mutant E11.5	< 2.2e-16	< 2.2e-16	x	119.6933	22.4702	83.444
wt E9	1.068E-11	3.929E-14	< 2.2e-16	x	732.8633	346.0525
wt E10.5	< 2.2e-16	< 2.2e-16	0.0000132	< 2.2e-16	x	54.4667
wt E11.5	< 2.2e-16	1.459E-09	< 2.2e-16	< 2.2e-16	1.488E-12	x

Figure 5. Loss of Notch in the ventral midline in *Foxa2^{T2AiCre}; Rosa26$^{LSL\text{-}dnMaml1}$* mice modifies cell fate. (A-H) Sections of spinal cord at lumbar level of E9 (A,B) E10.5 (C,D, G, H) or E11.5 (E,F)

Foxa2^{T2AiCre}*; Rosa26*$^{LSL\text{-}dnMaml1}$ mutants (scale bar=30 µm). (A-F) Sections analysed for Foxa2 and Nkx2.2. (G-H) Sections analysed for ARX. (I) Bar-chart showing changes in proportions of cells positive for either Foxa2 (red = early floor plate), Nkx2.2 (green = P3 progenitor) or Foxa2^{+}/Nkx2.2^{+} (orange = midline cells that may become floor plate or P3) within the ventral neural tube of E9 (A,B) E10.5 (C,D, G, H) E11.5 (E,F) *Foxa2*^{T2AiCre}*; Rosa26*$^{LSL\text{-}dnMaml1}$ mutants. The number/location of Foxa2^{+}/Nkx2.2^{+} cells (white dots) changes in the mutant at E9 and E10.5. The table presents Chi squared values in top right hand diagonal and *p*-value in bottom left hand diagonal. Sections counted: E9 WT=40, mutant=16; E10.5 WT=25, mutant=16; E11.5 WT=32, mutant 25.

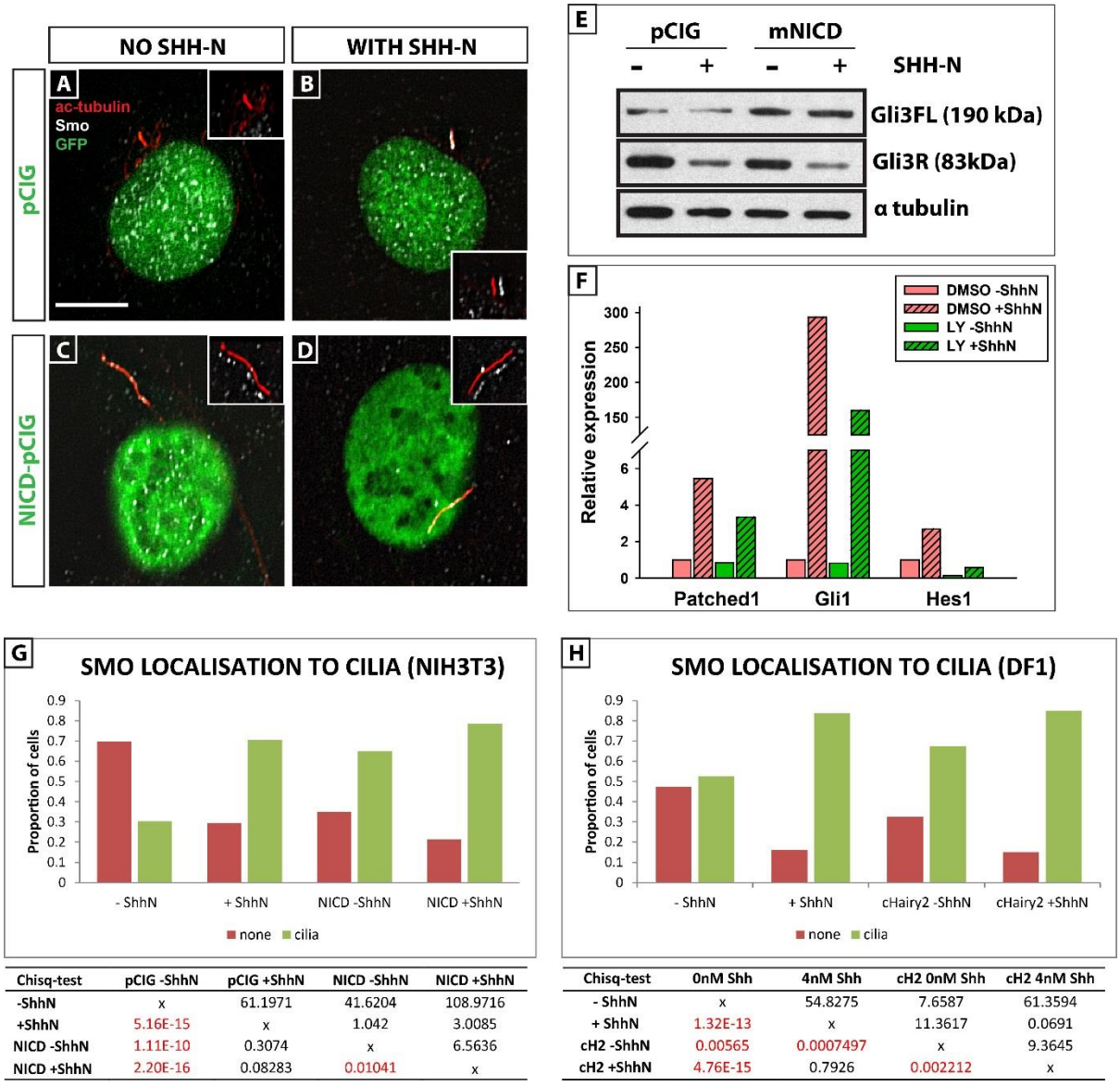

Chisq-test	pCIG -ShhN	pCIG +ShhN	NICD -ShhN	NICD +ShhN
-ShhN	x	61.1971	41.6204	108.9716
+ShhN	5.16E-15	x	1.042	3.0085
NICD -ShhN	1.11E-10	0.3074	x	6.5636
NICD +ShhN	2.20E-16	0.08283	0.01041	x

Chisq-test	0nM Shh	4nM Shh	cH2 0nM Shh	cH2 4nM Shh
- ShhN	x	54.8275	7.6587	61.3594
+ ShhN	1.32E-13	x	11.3617	0.0691
cH2 -ShhN	0.00565	0.0007497	x	9.3645
cH2 +ShhN	4.76E-15	0.7926	0.002212	x

Figure 6. Notch promotes cilia localisation of Smo in a Shh-independent manner. (A-D) NIH3T3 cells transfected with pCIG-GFP (A,B) or NICD-pCIG-GFP (C,D) in the presence (B,D) or absence (A, C) of Shh-N. pCIG–GFP or NICD-pCIG-GFP (green); cilia labelled with α-acetylated tubulin (red); Smoothened antibody staining in white. Scale bar=8 μm. (E) Western blot showing levels of full-length Gli3 (Gli3FL) and partially proteolysed repressor form (Gli3R) in cells transfected with pCIG–GFP or NICD-pCIG-GFP in presence/absence of ShhN. (F) qRT-PCR analysis of *Patched 1, Gli1 and Hes1* mRNA levels in NIH3T3 cells in the presence of DMSO, DMSO + Shh-N or LY + Shh-N. (G, H) Quantification of NIH3T3 (G) or DF-1 cells (H) depicting the proportions of cells that showed no smoothened (Smo) in cilia (red) *versus* cells that showed Smo localization in cilia (green) under different conditions. Cells transfected with NICD-pCIG-GFP had significantly longer cilia than pCIG-GFP transfected cells independent of ShhN (C,D versus A,B). Tables: Chi squared values in top right hand diagonal, *p*-value in bottom left hand diagonal. Significant results highlighted in red.

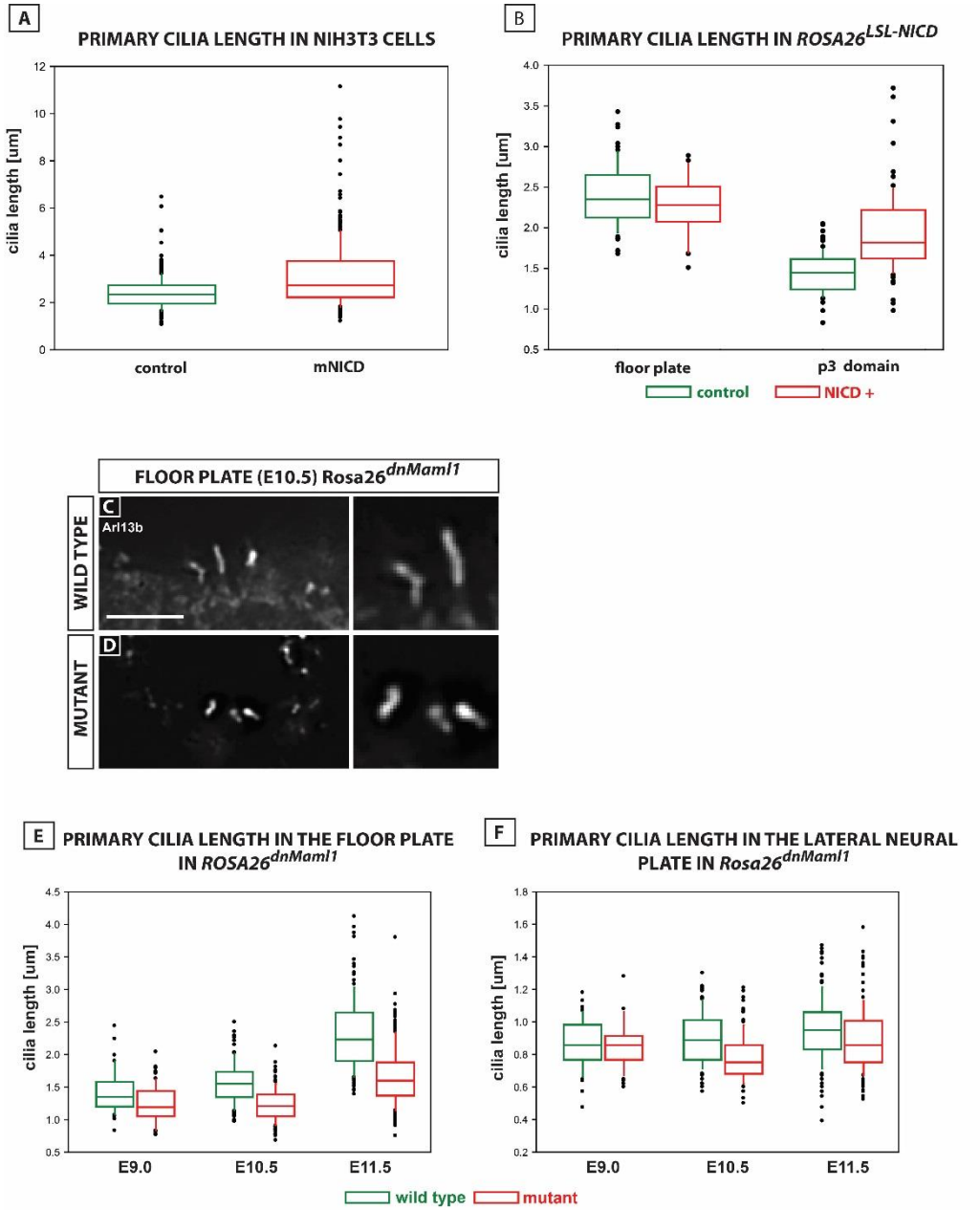

Figure 7. Notch regulates cilia length. (A, B) Quantitation of cilia length; box plots show median and range in NIH3t3 cells in presence/absence of NICD-pCIG-GFP (A), in floor plate and P3 domain of *Foxa2*^{mcm}*;Rosa26*$^{LSL\text{-}NICD}$ mutants (NICD+) *versus* control litter mates (B). (C-D) Cilia labelled with Arl13b antibody in the floor plate of *Foxa2*^{T2AiCre}*; Rosa26*$^{LSL\text{-}dnMaml1}$ mutant (D) versus wild type litter mate (C), Scale bar = 5 µm. (E-F) Quantitation of cilia length in floor plate and lateral neural plate of *Foxa2*^{T2AiCre}*; Rosa26*$^{LSL\text{-}dnMaml1}$ mutants (E9 *n*=3, E10.5 *n*=3 and E11.5 *n*=2) *versus* controls (E9 *n*=5, E10.5 *n*=2 and E11.5 *n*=2). Box plots show median and range; analysed by ANOVA. There is a highly significant three way interaction between cell type (floor plate and P3), developmental stage (E9, 10.5, 11.5), and genotype (mutant/control) at the *p*=<0.01level ([F(2,1354)=5.27, *p*=0.00525).

Table 1: Post-hoc pairwise comparisons using the Tukey HSD test to compare cilia length in Floor plate and P3 domains in *Foxa2*^{T2AiCre}; *Rosa26*$^{LSL\text{-}dnMaml1}$ and *Foxa2*^{mcm};*Rosa26*$^{LSL\text{-}NICD}$ mutant embryos versus wild type litter mates

Rosa26$^{LSL\text{-}dnMaml1}$ versus wild type	Difference in cilia length	Lower limit	Upper limit	Adjusted p-value
E9 P3	0.003687	-0.1207	0.128075	1
E9 FP	-0.15237	-0.27676	-0.02799	0.003682
E10.5 P3	-0.14352	-0.23154	-0.05551	7.1×10^{-6}
E10.5 FP	-0.25416	-0.34218	-0.16615	2.2×10^{-16}
E11.5 P3	-0.06368	-0.14389	0.016532	0.2811
E11.5 FP	-0.33704	-0.41725	-0.25683	2.2×10^{-16}
Foxa2^{mcm};*Rosa26*$^{LSL\text{-}NICD}$ versus wild type				
E10.5 FP	-0.11615	-0.34688	0.114577	0.5624687
E10.5 P3	0.477011	0.329829	0.624193	2.2×10^{-16}

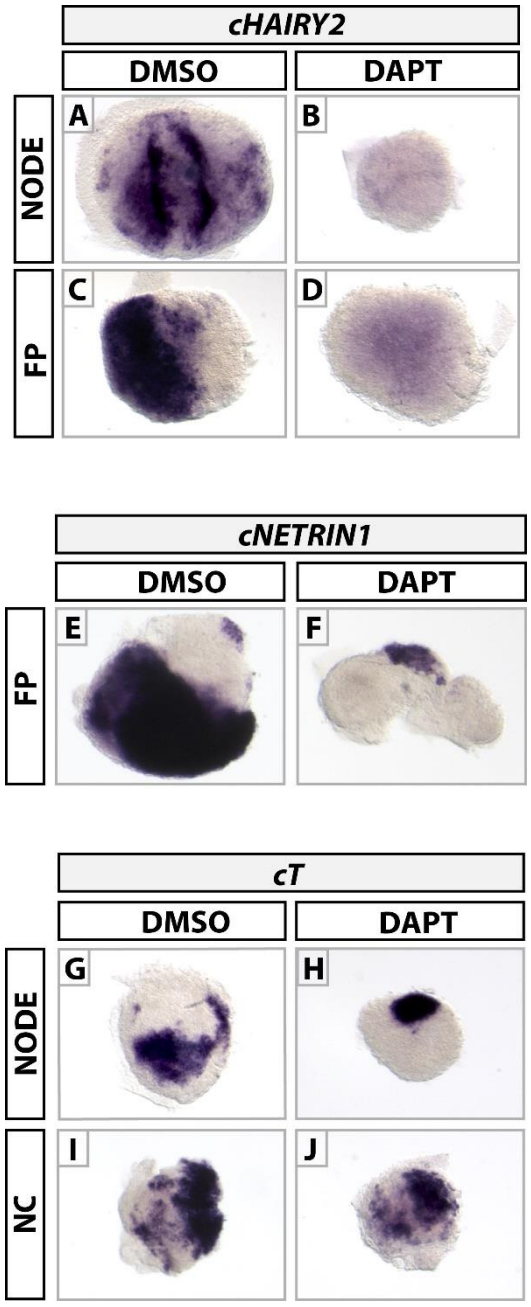

Supplementary Figure 1.

HH6/7 explants cultured in DMSO (A,C,E,G,I) or DAPT (B,D,F,H,J) analysed for *cHairy2* (A-D), *cNetrin1* (E-F), *cT* (G-J). *cHairy2* in Hensen's node (node) and floor plate (FP) (A,C) is down-regulated by DAPT (B,D). (E) FP cultured *in vitro* retains *cNetrin 1* expression, *n*=10/11. However, this is lost in the presence of DAPT (F). (I,J) Notochord (NC) expression of *cT* is unaffected by DAPT. *cT*; *cBrachyury*. Same magnification used for all images.

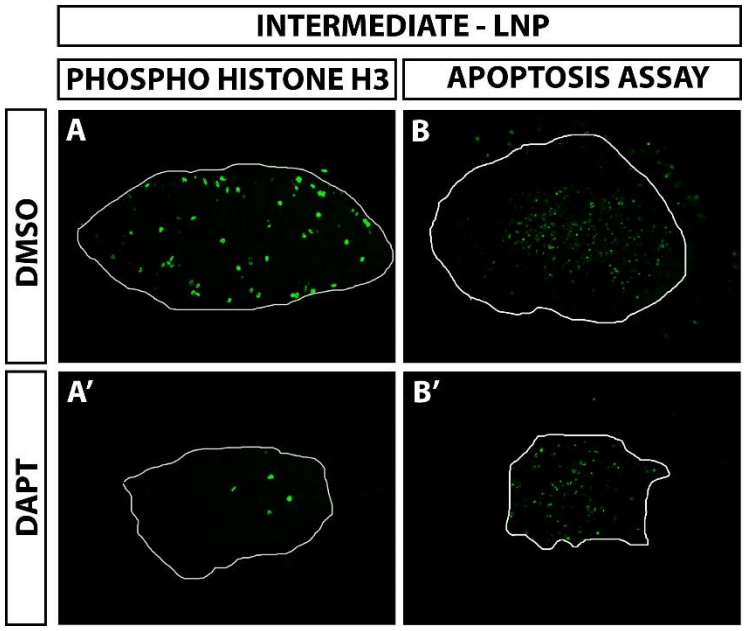

Supplementary Figure 2.

Sections from isolated neuroectoderm from HH6/7 embryos cultured in DMSO (A-B) or DAPT (A'-B'). Samples analysed with phospho histone-H3 antibodies (A, A') or the *In Situ* Cell Death Detection Kit (B, B').

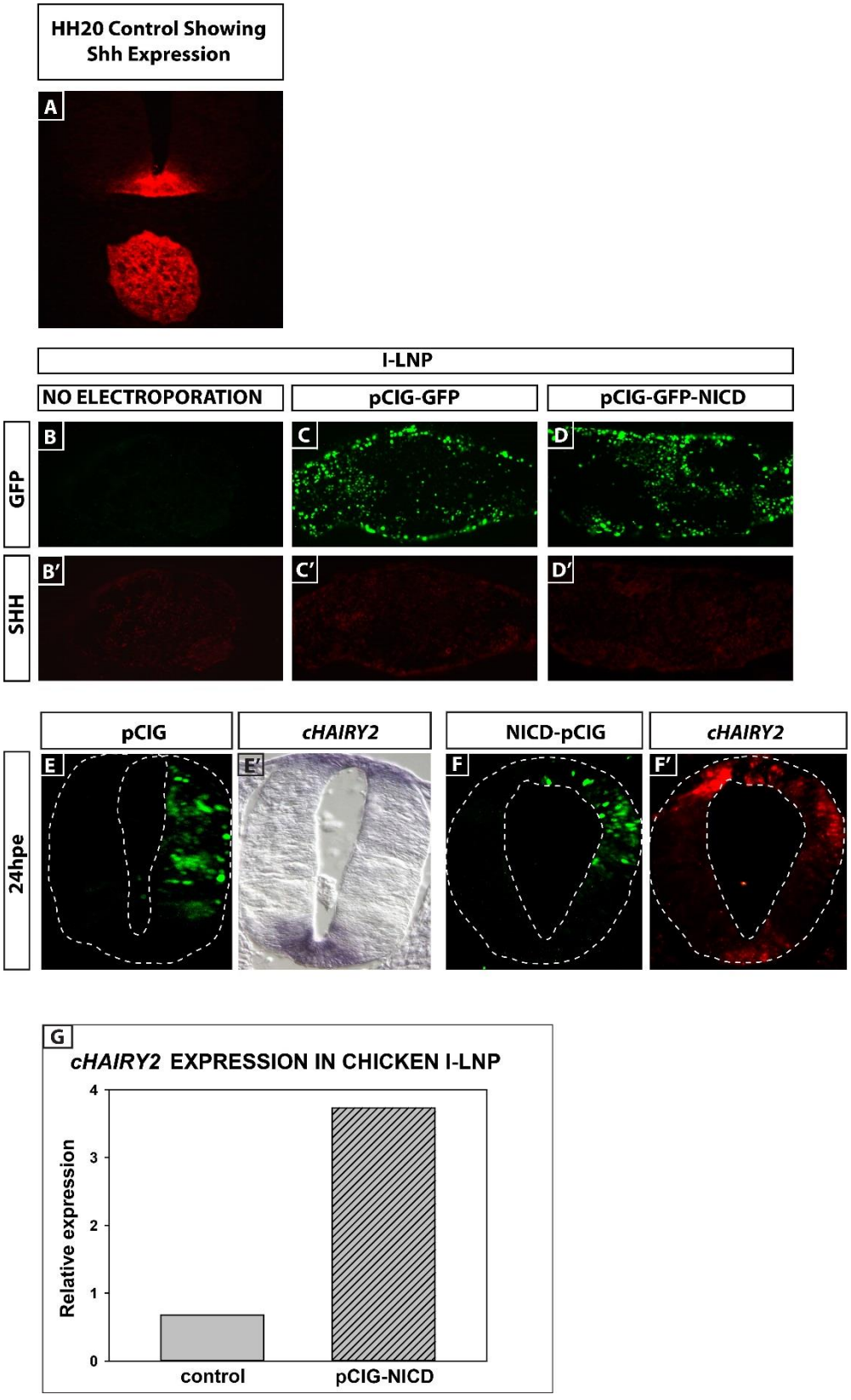

Supplementary Figure 3.

A) Shh expression in a transverse section of a control HH stage 20 chick embryo. B, B') A section of an isolated intermediate lateral neural plate (I-LNP) explant cultured alone, showing Shh is not

normally expressed by this tissue. C) A I-LNP section following electroporation with pCIG-GFP empty vector showing GFP-expressing cells throughout the explant. C') The same section as C, showing no Shh expression. D) A I-LNP section following electroporation with NICD-pCIG-GFP, showing GFP-expressing cells throughout the explant. D') The same section as D, showing that following NICD electroporation there is no induction of Shh. Sections were analysed by double immunohistochemistry for GFP and Shh expression. (E-F') Transverse sections of HH 17 chick neural tube 24 hours after electroporation with pCIG (E,E') or pCIG-NICD (F,F') analysed by regular or fluorescent in situ hybridisation for *cHairy2* expression. (G) qRT-PCR analysis of *cHairy2* mRNA levels, normalised to B-actin, in I-LNP explants electroporated with either control empty vector (pCIG) or pCIG-NICD.

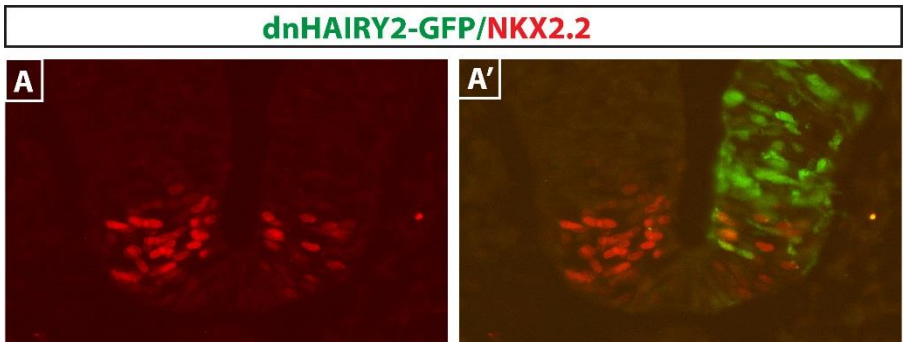

Supplementary Figure 4. (A-A') Transverse sections of HH 17 chick neural tube 24h after electroporation with pCIG-dominant-negative cHairy2 into the ventral midline (dnHairy2-GFP) (scale bar= 15µm). Sections were analysed for GFP and Nkx2.2 expression.

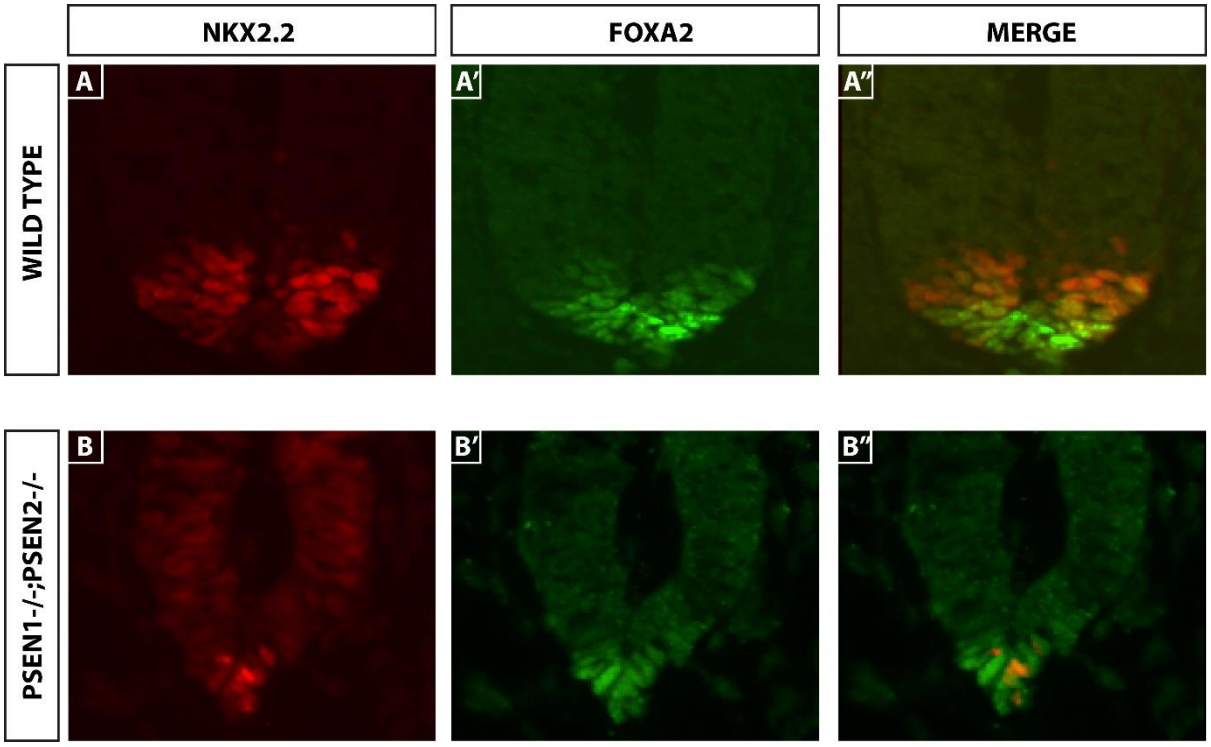

Supplementary Figure 5. (A-B') Transverse sections of neural tube of E9 *Psen1*$^{-/-}$*; Psen2*$^{-/-}$ mouse embryo (A-A'') and wild type litter mate (B-B''). Sections were analysed for Nkx2.2 and Foxa2 expression. The right-hand panels show the merged image.

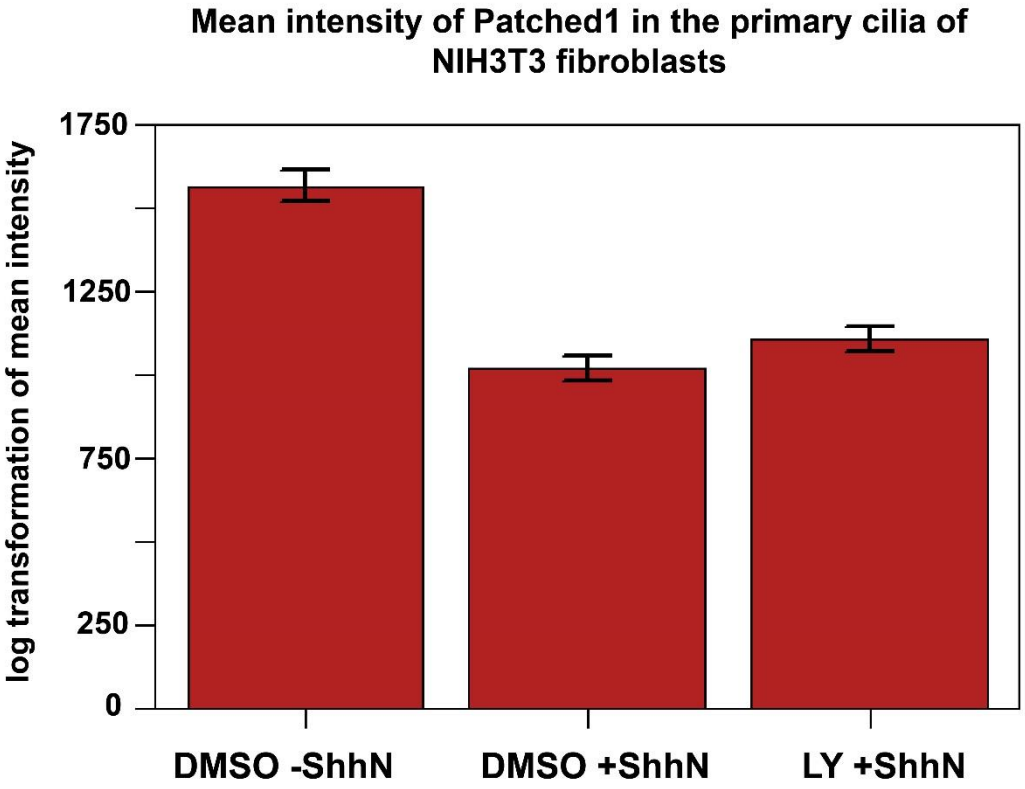

	df	Sum of squares	Mean square	F value	Significance
Between groups	2	45.43	22.716	176.5	$<2 \times 10^{-16}$
Within groups	1205	155.11	0.129		

	Difference	Lower bound	Upper bound	P value adjusted
DMSO +ShhN vs DMSO –ShhN	-0.45535195	-0.51532222	-0.3953817	<0.0005
LY +ShhN vs DMSO –ShhN	-0.36351561	-0.42303257	-0.3039987	<0.0005
LY +ShhN vs DMSO +ShhN	0.09183634	0.03320675	0.1504659	0.0007238

	Mean	95% ci
DMSO –ShhN	1566	+/- 45.3
DMSO +ShhN	1017	+/- 36.2
LY +ShhN	1109	+/- 37.8

Supplementary Figure 6. Bar chart plotting log transformation of PTC fluorescence intensity in cilia of NIH-3T3 cells cultured in DMSO, DMSO + 4 nM ShhN, or 150 nM LY + 4 nM ShhN. The region of interest was identified by expression of Arl13b, a specific marker of primary cilia. The min, max and mean intensity values for Patched1 signal were measured in Volocity software (PerkinElmer). For statistical analysis, the mean values were log transformed and compared using ANOVA (see below for table) and Tukey's Honest significant difference test (table can be seen below ANOVA table). There was a very highly significant effect for treatment, $F(2, 1205)=176.5$, $P<0.001$.